

## Deklim Schlussbericht

---

**ZE:** Institut für Küstenforschung, GKSS

**Förderkennzeichen:** 01LD0044

---

**Vorhabebezeichnung:** Rekonstruktion des Europäischen Klimas für die Instrumentelle Periode mit Hilfe von Datenassimilation durch Upscaling and Nudging (DATUN).

---

**Laufzeit des Vorhabens:** 01.01.2002 – 31.12.2004

---

**Martin Widmann, Julie M. Jones, and Eduardo Zorita.**

### Table of Contents

I. Kurze Darstellung zu:	
I.1 Aufgabenstellung	2
I.2. Voraussetzungen, unter denen das Vorhaben durchgeführt wurde	2
I.3. Planung und Ablauf des Vorhabens	3
I.4. wissenschaftlichen und technischem Stand an den angeknüpft wurde	4
I.5. Zusammenarbeit mit anderen Stellen	5
II.  Eingehende Darstellung:	
II.1. Erzieltes Ergebnis	5
II.1.1. Upscaling results	5
II.1.1.1 Northern Hemisphere Upscaling	6
II.1.1.2. Southern Hemisphere Upscaling	10
II.1.2. Pattern Nudging Results	16
II.1.2.1. Method Overview	16
II.1.2.2. Experiment Overview	18
II.1.2.3. Experiment design and definition of target fields	18
II.1.2.4. Results of nudging towards constant target amplitudes	23
II.1.2.5. Pattern nudging towards transient target amplitudes	29
II.2. Voraussichtlicher Nutzen insbesondere der Verwertbarkeit des Ergebnisses im Sinne des fortgeschriebenen Verwertungsplans	30
II.3. Während der Durchführung des Vorhabens dem ZE bekannt gewordener Fortschritts auf dem Gebiet des Vorhabens bei anderen Stellen	30
II.4. Erfolgte oder geplante Veröffentlichungen des Ergebnisses nach Nr. 11.	30
References	31

## **Section I**

### **I.1. Aufgabenstellung**

The detection of climatic changes during the last century and their attribution to forcing factors, including the increasing concentrations of atmospheric greenhouse gases, requires a realistic estimation of the magnitude of natural climate variability on decadal and longer time scales. Such estimates can be obtained in two ways: from palaeoclimatic proxy data, such as tree rings, varved sediments and corals, and from simulations with numerical climate models. Consistency tests between empirical and simulated climate estimates (e.g. Jones et al. 1998, Zorita et al. 2004) can reduce uncertainties, and contribute to the validation and improvement of climate models.

In palaeoclimatology climate models have been so far mainly used in two different ways. In quasi-equilibrium experiments the forcing factors for the climate system, such as solar radiation, the atmospheric composition, or the earth's orbit, are held constant, but may vary between different simulations. These simulations represent the mean climate and the statistics of internally generated climate variability consistent with the forcings. Transient, forced simulations additionally include the climate response to the estimated time-dependent forcings. Because of internal variability the evolution of the climate system is not completely determined by external forcings, even a perfect model, with all forcing mechanisms included, will yield only one out of many possible climate realizations consistent with the forcings. This realization will in most cases be different from the realization that took place in the real world, and any comparison between model and reconstruction will be therefore be probabilistic in nature.

In contrast to equilibrium and forced simulations, GCM runs in assimilation mode attempt to simulate the past climate as accurately as possible, including components of the historical time evolution of the quasi-random variability, that was internally generated by the dynamics of the climate system. The DATUN (Data Assimilation Through Upscaling and Nudging, von Storch et al. 2000a, Jones and Widmann 2004a) methodology is a new approach to use a GCM to assimilate information derived from proxy and long instrumental records. It consists of an upscaling step, in which large-scale circulation is derived statistically from empirical data, followed by an assimilation step in which the atmospheric states in a climate model are forced to be consistent with the empirical estimates.

This aim of this project is the assimilation of upscaled estimates of past atmospheric circulation from long instrumental records into the ECHAM4/HOPEG (ECHO-G) coupled atmosphere-ocean GCM. These upscaled estimates are more accurate than those obtained from proxy data, firstly because the instrumental records are based on direct measurements, and secondly, because the relationship with pressure is not based on an indirect relationship through temperature or precipitation, as in the case of proxy data. Thus the simulations can be used to test the pattern nudging, and if the method is successful, should provide a 3-dimensional 'reconstruction' of climate during the instrumental period.

### **I.2. Voraussetzungen, unter denen das Vorhaben durchgeführt wurde**

The palaeoclimate group at the GKSS has experience of climate modelling with the ECHO-G model (in non-assimilation mode), having undertaken a number of equilibrium and historical externally forced climate simulations for the past 500-1000 years (e.g. Zorita and Gonzalez-Rouco 2002, Zorita et al. 2003). First steps were also made during the KIHZ project in developing the theory behind pattern nudging and early implementation in the ECHAM4 GCM (Jones and Widmann 2004a). The group has also considerable experience of statistical climatology (von Storch and Zwiers 1999, Jones and Davies 2000, Zorita and von Storch, 1999, Widmann et al. 2003), and experience of upscaling of proxy and long instrumental data to produce climate reconstructions (Jones and Widmann 2003).

### I.3 Planung und Ablauf des Vorhabens

The milestones of the project formulated in the proposal are

- 1.) Derivation of statistical upscaling models for the long instrumental records. Following the concepts developed on KIHZ, this will be mainly based on Canonical Correlation Analysis between the instrumental records and atmospheric data from the NCEP/NCAR reanalysis, but if necessary other type of models, possibly non-linear will be explored.
- 2.) Application of these upscaling models to estimate large-scale climate anomalies from the mid-19<sup>th</sup> century to the present.
- 3.) Assimilation runs with the fully coupled ECHO-G model.
- 4.) Validation of the reconstruction based on three criteria:
  - a.) Are the surface observations reproduced?
  - b.) Is the reconstruction after 1948 consistent with the NCEP/NCAR reanalysis? This reconstruction will include upper-air fields
  - c.) What is the space- and time-dependent spread of the ensemble?
  - d.) How are the high-frequency (weather) statistics modified in comparison with the observations and non-assimilated runs?

(There is also a milestone 5 in the proposal, but this seems to be erroneously included from a draft version, as it is practically identical to milestone 4)

Milestones 1 and 2 have been reached as planned, as we have reconstructed the amplitudes of the dominant circulation modes in both hemispheres (Arctic and Antarctic Oscillation, (A)AO) for all seasons in the Southern Hemisphere (SH) back to at least 1905, and for most seasons back to around 1870 in the Northern Hemisphere (NH). The reconstructions for the SH go somewhat beyond the original plans which included only NH reconstruction. This extension of the project was based on the realization that SH reconstructions would be highly desirable for assimilation simulations, have a scientific value on their own, as can be seen by two publications in high-ranked journals on this topic (Jones and Widmann 2003/2004b), and were not yet attempted by other groups but feasible to be produced with the data and methods available to our group.

With respect to milestones 3 and 4 we have conducted and analysed more than 50 different assimilation simulations. However, we have not yet fully completed these milestones for several reasons. It became evident during the early phase of the project that the implementation of the pattern nudging assimilation method in ECHAM4 was not yet operational. Several errors in the original implementation were identified and corrected, and many simulations have been run in order to optimise the specific setup. During the project the pattern nudging module for ECHAM4, as well as the code to produce the input files, were completely rewritten, in order to make them less error prone, more flexible, and more user friendly. We also needed to do additional analysis on differences between the ECHAM4 model and reality (NCEP) in the circulation structure, as well as on the relation between the vorticity in the free troposphere (which is nudged) and the sea level pressure (SLP) field. Moreover, we had to solve problems related to the exact formulation of the statistical link between target indices (such as the AO index) and their associated structure in the vorticity field, which is used for the nudging. This work led to a publication in Journal of Climate (Widmann 2005). Because of these unexpected problems some of the originally planned analysis had to be postponed. As we were still optimising the pattern nudging code, we used the ECHAM4 atmosphere model without the coupling to the ocean in order to save computing time. The pattern nudging module has however been successfully compiled with the coupled model and we do not expect any additional problems when running the coupled model.

Most of the validation of pattern nudging (milestone 4) has so far been based on test simulations in which the circulation in ECHAM4 was nudged towards constant target values of the AO index (AOI). Typical results are described in section II and are currently being written up for submission to *Climate Dynamics* (Widmann et al. 2005). We have also completed a transient simulation for the period 1948-2002 in which the AOI in ECHAM4 is nudged towards the real world AOI derived from the NCEP reanalysis. A first analysis shows that the nudging allows control of the AOI as desired. An extension back to the 19<sup>th</sup> century using our (A)AOI reconstructions poses no additional technical problems and we plan to start such a simulation (with the coupled model) in late 2005/early 2006, after we have undertaken a more fully comparison of the transient nudged simulation with the NCEP reanalysis. Exact timing of when this simulation will be started, and the analysis undertaken, depends on commitments to other projects for which Julie Jones and Martin Widmann are Principal Investigators, and by which they are funded. This analysis will cover milestones 4a and 4b, which are at the moment not covered by our analysis. Milestone 4c is partly addressed by the analysis of the simulations towards constant target amplitudes, as this shows how much the simulation varies when there is no change in the target amplitudes for the nudging. Milestone 4d has been covered by a comparison of the synoptic-scale variability in nudged and non-nudged simulations.

It should be pointed out that the pattern nudging is a completely new area of model development for which no previous experience from any research groups is available. Although we encountered some unexpected problems, we are systematically progressing towards providing an operational new tool for palaeoclimatic research and dynamical analyses. The remaining work needed to cover all milestones of the project is continued in our group in close cooperation with the Max-Planck-Institute for Meteorology.

#### **I.4 Wissenschaftlicher und technischer Stand an den angeknüpft wurde**

The climate model used, is the ECHAM4 atmospheric model (Roeckner et al. 1996) coupled to the HOPE-G ocean model (Wolff et al. 1997), together called ECHO-G (Legutke and Voss 1999). A transient simulation forced with historical estimates of past forcing factors, as well as a 1000 year control simulation had been carried out at the GKSS with this model (Zorita et al. 2004, Zorita and Gonzalez-Rouco 2002). The pattern nudging is a new method whose development started during the KIHZ project. The first publication on pattern nudging is von Storch et al. (2000a). The results of the first steps on DATUN in the KIHZ project are documented in Jones and Widmann (2004a).

Some of the earliest work on upscaling of point data to produce large-scale reconstructions was undertaken in the tree-ring community (e.g. Fritts et al. 1971, Schweingruber et al. 1991, Briffa et al. 2001). With the development of multiproxy reconstructions, long instrumental series have also been included as predictors in reconstructions together with proxy data, e.g. for circulation indices (Luterbacher et al. 1999, Cullen et al. 2001) and climate fields (Luterbacher et al 2000, Mann et al. 1998, 1999). Comparison of different proxy-based NAO index reconstructions showed inconsistencies, perhaps due to non-stationarities in the statistical relationships between the proxy data and the NAO (Schmutz et al. 2000). Jones and Widmann (2003) was the first study to our knowledge to use only instrumental data for a circulation index reconstruction. Jones et al. (1999a) used long station pressure records to reconstruct European pressure for the period 1780-1995.

## **I.5 Zusammenarbeit mit anderen Stellen**

The implementation of the pattern nudging into the ECHAM4 GCM has been done in collaboration with Reiner Schnur from the Max-Planck-Institute for Meteorology (MPI) in Hamburg, and with Ingo Kirchner from the Free University of Berlin (formerly MPI). Collaboration on implementing pattern nudging into the Hadley Centre climate model together with the Climatic Research Unit, Norwich, UK and the Hadley Centre, shall begin in late 2005.

For the reconstructions, data has been provided from the Climatic Research Unit, Norwich, UK (Phil Jones), and from the Hadley Centre, UK (Rob Allan and Tara Ansell). Rob Allan has also provided us with a beta version of the HadSLP2 dataset, a global gridded SLP dataset on a 5 degree by 5 degree grid. At present we have permission only to use this dataset for investigation of the AAO, thus it has not been used in the NH analysis. Through Rob Allan, Julie Jones has been invited to attend a meeting of the Global Climate Observing System (GCOS) surface pressure working group (<http://www.cdc.noaa.gov/Pressure/>) in October 2005.

An annual AAOI reconstruction has been produced as part of a collaboration with Dave Schneider of the University of Washington, Seattle (Schneider et al. 2004), as this is the season in which the AAOI has the highest correlation with stable isotopes from a network of Antarctic ice cores. This work has been unsuccessfully submitted to Science, and is under revision for submission to another journal. The results for the annual reconstruction are not shown here, as the seasonal behaviour is more informative, and annual reconstructions are not required for data assimilation.

## **Section II.**

### **II.1 Erzieltes Ergebnis**

The upscaling results shall first be described, for the NH and then the SH. The results of the pattern nudging shall then be described. The development of methods and experimental set up are explained in some detail for the pattern nudging, as this comprised a major part of the research.

#### **II.1.1. Upscaling Results**

The first mode of extratropical atmospheric circulation variability in each hemisphere has been reconstructed. In the NH this is the so-called Arctic Oscillation (AO), and in the SH the Antarctic Oscillation (AAO). Together these are known as the Northern Hemisphere and Southern Hemisphere Annular Modes (Thompson and Wallace 2000). They are zonally symmetric modes, representing exchange of mass between the mid and high latitudes, and characterise fluctuations in the strength of the circumpolar vortex (Thompson and Wallace 2000). They are commonly defined as the first EOF of extratropical sea level pressure (SLP).

Due to the larger amount of historical meteorological data in the NH, more is known about climate during the historical period here than in the SH. Gridded NH SLP data is available from 1873 to present, although in the early period of this data uncertainties exist. In the SH, for most of the project period, no reliable gridded hemispheric data existed prior to the period for which reanalysis data exists (1948 for NCEP/NCAR reanalysis, 1958 for ERA40 reanalysis). Thus although the original project proposal concentrated on the NH, it became clear in the early stages of the project that much knowledge could be gained from both the atmospheric circulation reconstructions, and the assimilation simulations, in the SH prior to the second half of the 20<sup>th</sup> century. This is exemplified by the publication of the austral summer AAOI reconstruction in Nature (Jones and Widmann 2004b).

### *II.1.1.1. Northern Hemisphere Upscaling*

#### *Data and methods*

The predictand data were NCAR/NCEP reanalysis data. These data cover the period 1948-2003. For computational ease, they were regridded from the 2.5° by 2.5° grid (approximately 1.2 degrees by 1.2 degrees) to a 5° by 5° grid. As predictors, a dataset of SLP from 51 stations from the EU Advice project (Slonosky et al. 1999) were used. These were obtained from Phil Jones from the Climatic Research Unit, Norwich, UK. Stations were included in the reconstructions that are significantly correlated at the 95% level with the detrended AOI. For model fitting we define the AOI as the first PC of detrended NCAR/NCEP seasonal mean SLP for the extratropical domain (20°N-90°N), and the AO as the first EOF of these data. We used multiple linear regression (von Storch and Zwiers 1999) to estimate the AOI from the leading principal components (PCs) of normalised station SLP (so-called principal component regression (PCR)). The PCR methodology is described in more detail in Jones and Widmann (2003) and the supplementary online material of Jones and Widmann (2004b). With one predictand, PCR is identical to canonical correlation analysis, the method outlined in the proposal.

The 95% confidence intervals for low frequency variability are shown on the reconstructions. The intervals are defined as  $\pm 1.96$  standard deviations of the residuals from the model fitting, because during the fitting period and for normally distributed residuals about 95% of the true AOI values lay inside an interval of this size. An additional, non-quantifiable uncertainty that is not contained in these confidence intervals stems from the fact that the relationship between local pressure and the AO outside of the fitting period may be different to that derived during the fitting period.

Reconstructions have been undertaken for 1871-1998 (where 51 stations are available), and a second for 1789-1998 (where 13 stations are available). Gridded hemispheric SLP data go back to 1871, but there are uncertainties in the early period, mainly due to the large influence of interpolation in data sparse regions. Our AOI reconstructions provide for the early period of the gridded data an alternative and internally consistent approach to calculating the AOI directly as PC1 of the gridded data. The two approaches can be compared to estimate the uncertainties in the AOI estimates. We only have permission to use the beta version of the HadSLP2 dataset for investigating the AAOI, thus the previous version, HadSLP1 is used for comparison with the reconstructed AOIs. We anticipate that we shall have access to the final version of HadSLP2 for undertaking the assimilation simulation if necessary.

#### *Results*

Figure 1 shows the AO in the four standard seasons: boreal winter (DJF), spring (MAM), summer (JJA) and autumn (SON). In some seasons the EOF loadings over Europe, where our data are located, are low. Thompson and Wallace (2000) also find lower regression coefficients between SLP over Europe and the AOI in the summer half year than in the winter half year. For example the maximum pressure change over Europe associated with a 1 standard deviation change in the AOI is 1hPa, compared to 2.5 hPa in DJF. Thus even in the centres of action, correlations with the station data will be lower (Table 1). Thus in JJA, no stations show a significant correlation with the AOI, and the reconstruction with the best validation statistics is DJF. In MAM and SON the correlations are strong enough for reconstructions to be undertaken back to 1871. In MAM the fitting and validation revealed that the 8 stations that were selected by the pre-filtering for the 1789 reconstruction could not produce a reconstruction with reasonable fitting and validation statistics (Table 1). Thus no long reconstruction was undertaken in this season. Given the reasonable validation over the 1871-1998 period, the possibility of an intermediate length reconstruction shall be investigated for assimilation in the historical transient simulation.

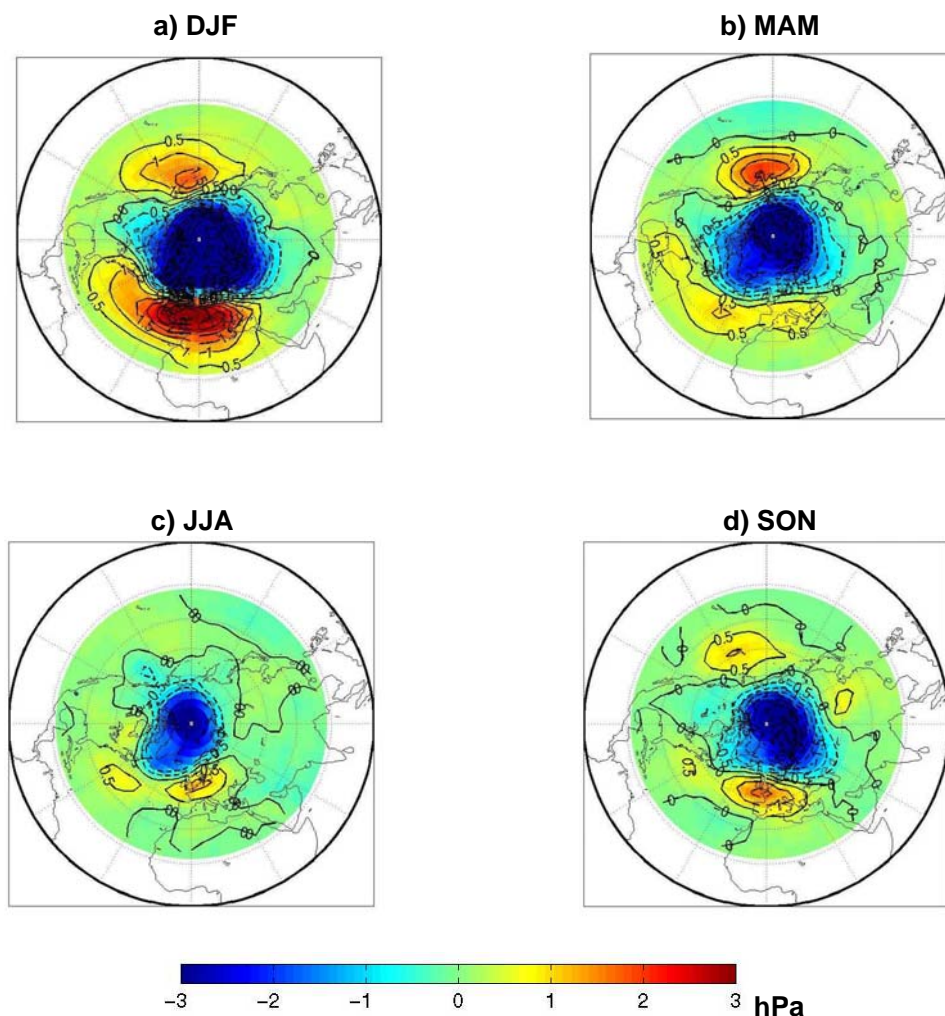


**Figure 1.** The Arctic Oscillation in boreal a) winter, b) spring, c) summer and d) autumn. The scale shows the change in surface pressure for a 1 standard deviation change in the Arctic Oscillation Index.

We compare the reconstructed AOIs against those calculated from two datasets: based on the data of Trenberth and Paolino (1980), and that calculated from the HadSLP1 gridded dataset, which is an update of the GMSLP2 dataset (Basnett and Parker 1997) – hereafter termed the gridded AOIs. Figure 2 shows that agreement between the reconstructed and gridded AOIs are best in DJF, with a correlation between the Trenberth AOI and the 1871 (1789) reconstructions of 0.88 and 0.90 respectively for the 9-year filtered data, and of 0.81 and 0.80 respectively for interannual data. This reflects the strong correlation between the stations and the AOI in this season, due to the strong AO signal over Europe. In MAM, agreement is reasonable, correlations between the Trenberth AOI being 0.86 and 0.81 for the filtered and interannual data respectively. This suggests that an intermediate length reconstruction (longer than 1871, shorter than 1789) may be achieved. Correlation between the SON AOIs and the gridded AOIs are weaker, strongest correlations are with the HadSLP1 dataset: 0.50 and 0.21 for the 1871 and 1789 reconstructions respectively for the filtered data, and 0.70 and 0.50 for the interannual data.

season	calibration period correlation		validation period correlation		Reduction of error		Number of stations		% of SLP variance explained by the AO	maximum station correlation with detrended AO
	1871	1789	1871	1789	1871	1789	1871	1789		
<b>DJF</b>	0.90	0.90	0.89	0.89	0.81	0.81	42	8	36	0.80
<b>MAM</b>	0.83	0.44	0.78	0.37	0.61	0.13	33	8	33	0.60
<b>JJA</b>									32	0.25
<b>SON</b>	0.89	0.70	0.83	0.68	0.68	0.46	35	9	26	0.72

**Table 1.** The calibration and validation statistics for the seasonal AOI regression model, the number of stations included, and the percentage of sea level pressure variance explained by the AAO.

These results suggest that for the assimilation run, in DJF, instrumental reconstructions back to 1789 could be assimilated. In the other three seasons, the AOIs calculated from gridded data should be used for the later period (although it should be remembered that there will be uncertainties also in the gridded data earlier in the series). In MAM and SON it may be possible to extend the reconstruction prior to the period of gridded data, although obviously these reconstructions will have relatively large uncertainties associated with them. It is evident from Figure 2 that there are some differences between the gridded AOIs in the non-winter seasons. Advice shall be taken on which dataset could be used. Access to the HadSLP2 dataset could be achieved by then. Julie Jones is attending a meeting of the GCOS AOPC/OOPC surface pressure working group (<http://www.cdc.noaa.gov/Pressure/>) in October 2005, where this issue can be clarified.

Figure 3 shows the reconstructions for DJF, MAM and SON. In DJF, the interannual values of the reconstruction are shown for the long reconstruction. In SON, due to the greater uncertainties associated with the long reconstruction, the interannual values are shown for the 1871 reconstruction, and the filtered 1789 reconstruction shown (thick black line).

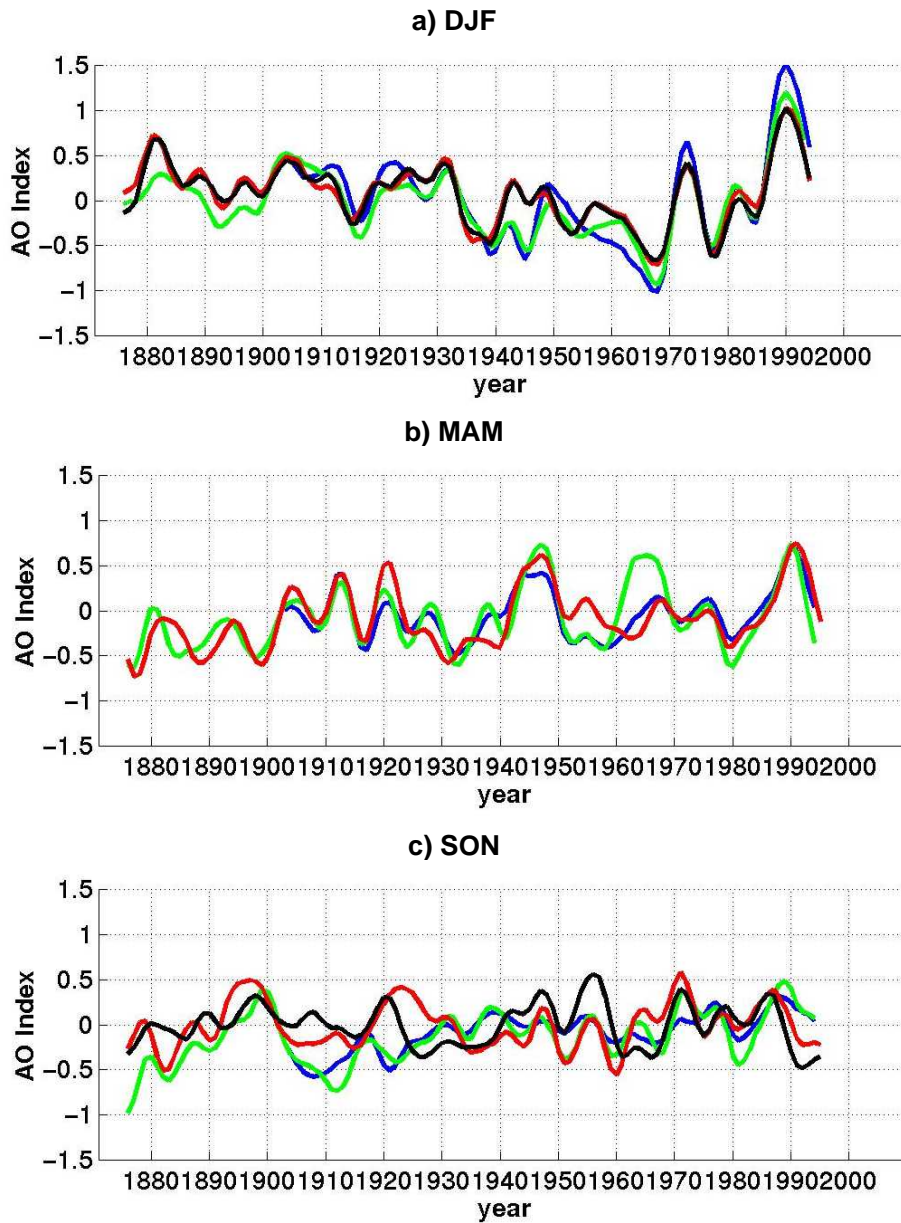


**Figure 2.** Reconstructed and instrumental 9-year filtered AOIs: Trenberth and Paolino (blue), HadSLP1 (green), 1871 reconstruction (red), 1789 reconstruction (black).

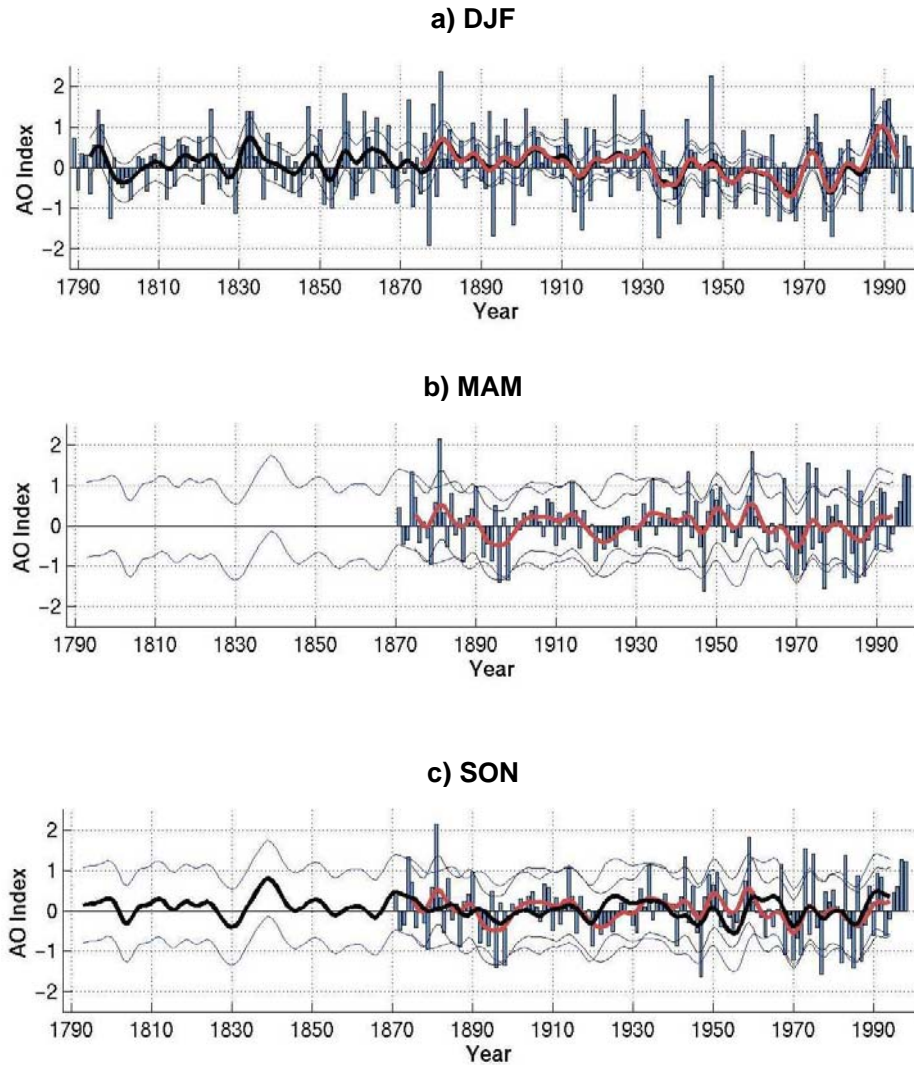


**Figure 3.** The AOI reconstructions. The blue bars are in a) DJF 1789 reconstruction, b) and c) the 1878 reconstructions. The thick black line is the 9-year filtered 1789 reconstruction, and the thick red line the 9-year filtered 1871 reconstruction. The thin lines are the low frequency 95% confidence intervals.

The reconstructions show that, as in the gridded data, and found by Thompson et al. (2000), the strongest positive AOI trend over the past 30 years is in the winter months. The trend is clearly evident in the nine-year filtered reconstruction in this season. Thompson et al. (2000) found positive, but not statistically significant (at the 95% level) trends in the other months. The nine-year filtered data show that the decadal-scale variability is greatest in the past decades in DJ than during the rest of the reconstruction. Many modelling studies indicate strengthening of the AO under climate change although the direction of change is not clear and at present model-dependent (Rauthe et al. 2004, Rind et al. 2005 a,b).

### ***II.1.1.2. Southern Hemisphere Upscaling***

We have undertaken reconstructions of the AAOI for austral winter (JJA), spring (SON), summer (DJ) and autumn (MAM). The reconstruction for DJ was undertaken as trends in this season have recently attracted much interest. In the past 2-3 decades there has been a trend in austral summer towards a positive AAO (stronger circumpolar westerly flow), that has been linked in this season to stratospheric ozone depletion. Studies investigating this trend have concentrated on anthropogenic stratospheric

ozone depletion (Thompson and Solomon 2002 (hereafter TS), Gillett and Thompson 2003 (hereafter GT) and greenhouse gas emissions (Stone et al. 2001, Kushner et al. 2001). Our work allows for the first time these recent trends to be put in a longer-term context, as hemispheric data is available only for the reanalysis period: NCEP/NCAR back to 1948, and the ERA40 to 1958. This work builds on the work of Jones and Widmann (2003), who undertook two reconstructions of the austral summer (November, December, January) AAO, one using station sea level pressure (SLP) measurements and another using tree ring-width chronologies, to estimate the AAOI back to 1878 and 1743 respectively.

To provide more accurate reconstructions for the last 50 years, shorter reconstructions utilising the greater number of available stations for the period 1951-2000 for all seasons were undertaken.

#### *Data and Methods*

The predictand data were ERA40 reanalysis data, obtained from the ECMWF. These data cover the period 1958-2003. These newer data may have less uncertainty in southern high-latitude climate than the old NCAR/NCEP reanalysis. For computational ease, they were regridded from the original N80 grid (approximately 1.2 degrees by 1.2 degrees) to a 5 degree by 5 degree grid.

SH station SLP records with data to 2001 were obtained from Phil Jones, Climatic Research Unit, UK (Jones et al. 1999b; Jones 1991). These data originate mostly from the World Weather Records and some earlier data from yearbooks from the UK National Meteorological Library at Bracknell, and have been homogenised according to Jones (1987). There are 41 stations in this dataset with data to at least 1905. Additional stations were provided by Rob Allan and Tara Ansell from the Hadley Centre (Allan and Ansell 2005). These provide additional stations with long records (at least to 1866), to enable longer reconstructions to be undertaken.

As for the AO reconstructions, we used PCR to estimate the AAOI from the leading PCs of normalised station SLP. For model fitting we define the AAOI as the first PC of detrended ERA40 seasonal mean SLP for the extratropical domain (20°S-80°S), and the AAO as the first EOF of these data. Uncertainties in the reanalysis data exist in the *non-summer* season (Bromwich and Fogt 2004) at high latitudes during the pre-satellite era. Thus in austral spring (SON), autumn (MAM) and winter (JJA), the period 1972-2001 was chosen for model fitting, as this is the period when satellite data has been assimilated in the reanalysis. In summer (DJ(F) the full period of reanalysis data (1958-2001) was used for model fitting.

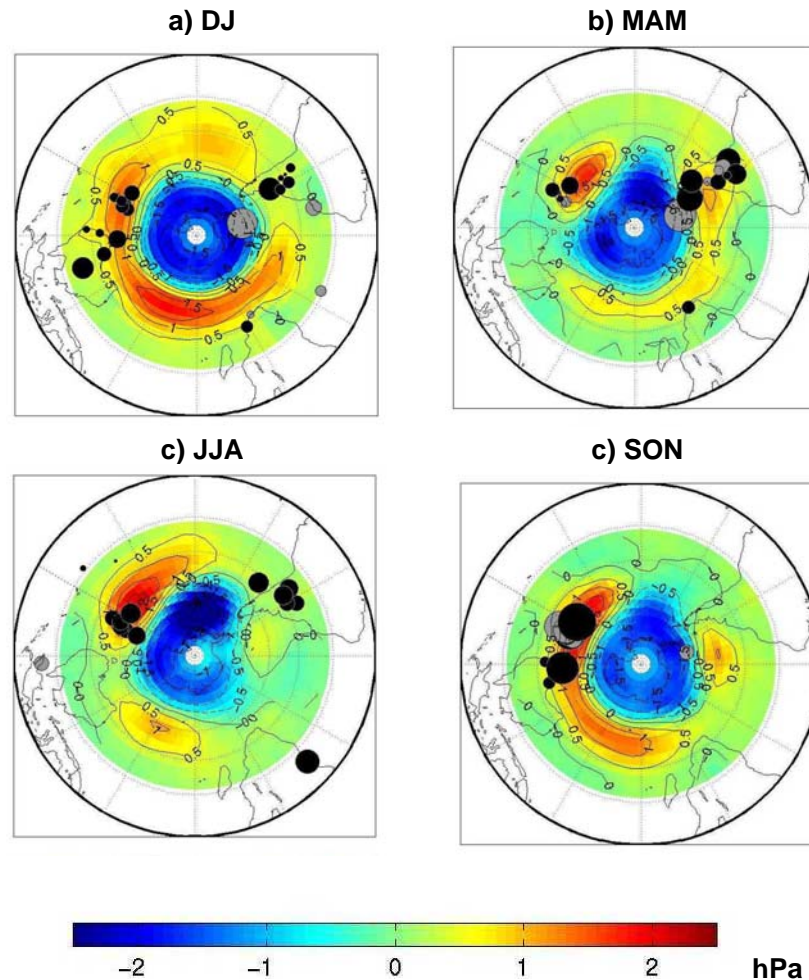
#### *Results*

Reconstructions have been produced for four seasons, JJA, SON, MAM, and DJ (DJF will be used for the assimilation, but results are very similar). One reconstruction was carried out from 1905-2001, and a second from 1951-2001. A larger number of stations are available from the latter period, most importantly data from the Southern Indian Ocean centre of action and more stations from the Antarctic centre of action, which are lacking for the longer reconstructions, are available during the latter period. In those season in which it is possible (DJ and MAM) a reconstruction back to 1866 has also been undertaken.

Season	calibration period correlation		validation period correlation		Reduction of error		number of stations		% of SLP variance explained by the AAO
	1905	1951	1905	1951	1905	1951	1905	1951	
<b>DJ</b>	0.91	0.91	0.88	0.90	0.77	0.81	22	41	42
<b>MAM</b>	0.88	0.88	0.84	0.84	0.69	0.70	19	28	27
<b>JJA</b>	0.84	0.83	0.82	0.82	0.66	0.66	11	13	28
<b>SON</b>	0.76	0.81	0.65	0.78	0.41	0.60	10	16	25

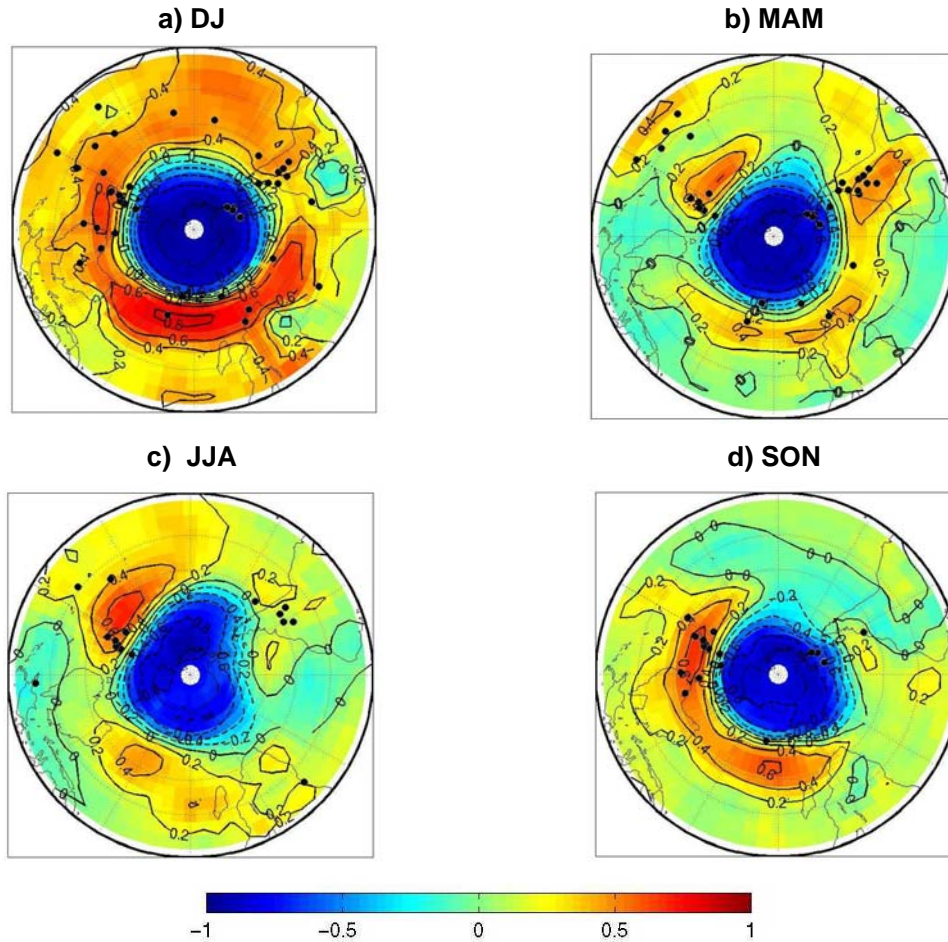
**Table 2.** The calibration and validation statistics for the seasonal regression models, the number of stations included, and the percentage of sea level pressure variance explained by the AAO.

Table 2 shows that the most stations were significantly correlated with the AAOI and thus used as predictors for both the 1905 and 1951 reconstructions in DJ. In MAM for the 1905 reconstruction, 17 stations were significantly correlated, all of which are located in the positive centre of action. The locations of the stations, and their regression weights for the 1905 reconstruction are shown in Figure 4.



**Figure 4.** The AAO pattern and the regression weights for normalised station sea level pressure (SLP) used for the 1951 AAOI reconstruction. Isolines show the SLP anomaly (hPa) for AAOI +1. The black (grey) circles denote positive (negative) values; the circle area is proportional to the weight.

In JJA and SON fewer stations are included in both the long and the short reconstructions. In JJA the fitting and validation statistics do not improve as only two extra stations are included. This is because of the differing spatial structure of the AAO in these seasons (Figure 4), and the differing proportion of SLP variance explained by the AAO (Table 2). The AAO explains the highest variance of the SLP data in DJ (42%). In the other seasons it explains between 24% and 28%. The AAO structure in DJ and MAM has more centres of action located over the continents and New Zealand than in JJA and SON. Figure 5 shows the correlation between ERA40 SLP and the AAOI in each season. In all seasons correlations over and around New Zealand are high, between 0.4 and 0.7. Over Southern South America, Southern Africa, in DJ, NDJ and MAM correlations are 0.4-0.6, i.e. the AAOI explains 16- 36% of local SLP variability. In JJA and SON the correlations are much lower in these areas (0.2, thus explaining 4% of SLP variance, so fewer stations from these regions are significantly correlated with the AAOI, and thus included in the reconstruction.



**Figure 5.** Correlation between detrended ERA40 AAOI and ERA40 SLP. The dots are the locations of the stations used for the 1951 reconstructions.

In DJ the AAO is very annular, with zonally oriented bands of positive loadings at mid-latitudes, and negative loadings at high-latitudes, with the zero line at around 50°S. In MAM the pattern is slightly less zonal, with low loadings extending northwards in the eastern Pacific to north of 45°S. The AAO is least zonal in SON and JJA, where in the southeast Pacific and in the south Atlantic the negative loadings extend northwards, but not in a zonally symmetric way, the AAO appears more as a wavenumber 3 pattern. Chen and Yen (1997) also noted such a pattern in winter at high middle latitudes. Rogers and van Loon (1982) also found that in winter the greater midlatitude anomalies are found over Chatham Island rather than over the central Indian Ocean as in summer.

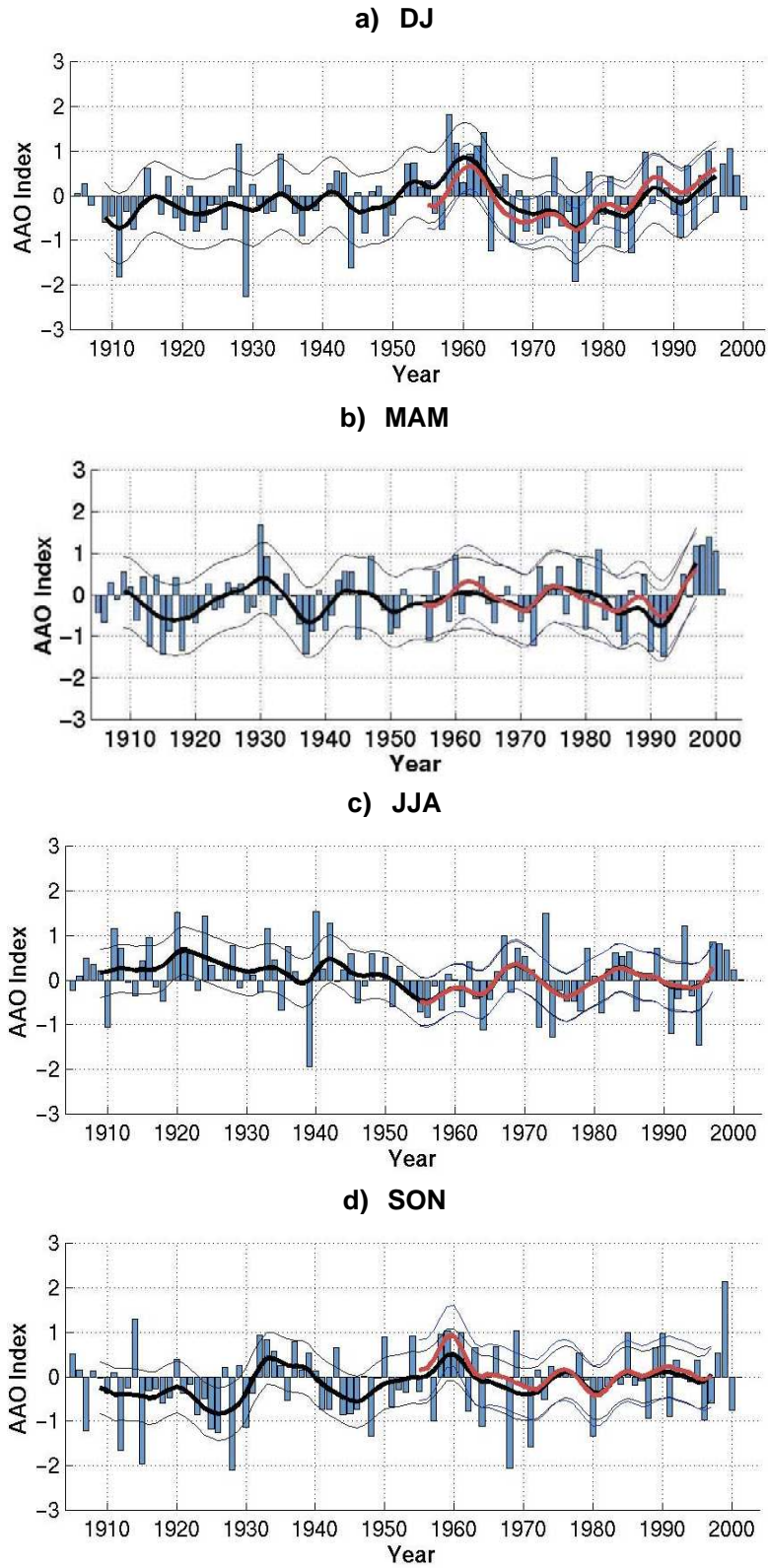


**Figure 6.** The reconstructed AAOI. Bars show the 1905 interannual reconstructions. The thick black line is the nine-year low-pass filtered 1905 reconstruction, the thick red line the filtered 1951 reconstruction. The thin lines are the 95% low frequency confidence intervals for the filtered data for the 1905 (blue) and 1951 (black) reconstructions.

The DJ behaviour of the AAOI is of particular interest as these are the months in which the index has been linked to stratospheric ozone depletion (TS, GT). This is also the season in which we can have most confidence in the reconstructions. The DJ reconstructions (Figure 6) show that the current positive AAOI values are not unprecedented (Jones and Widmann 2004b). After a relatively stable first half of the twentieth century, there is a period of positive values (relative to the 1958-2000 mean) from 1958-1963, followed by a sharp drop to dominantly negative values until the mid-1980s, and then by a mostly positive phase until present. The maximum positive 25-year trends over recent years are of similar magnitude to those between the low values in the 1940s and the 1960s peak. Note that the trend over the last decades is caused by a combination of negative values in the 1970s and positive current values.

A positive AAOI around 1960, followed by a negative index, is also present in the NCEP and the ERA40 data, in a zonal index based AAOI (Marshall 2003), in the SBR and the tree-based reconstruction of JW. Consistent with this AAO behaviour, station pressures around 1960 have positive anomalies in the mid-latitude centres of action and negative anomalies in the Antarctic centre of action. Unlike in our reconstructions, in both reanalyses and the zonal index AAOI the 1960s peak is slightly lower than the 1990s peak. Despite this small uncertainty about the exact values, the 1960s peak is a robust feature in all the above datasets. The strongly positive AAOI and large positive trend during a period before ozone depleting chemicals were emitted into the atmosphere and before strong anthropogenic warming occurred, together with the negative trend, suggest that natural forcing factors or internal mechanisms in the climate system must also strongly influence the state of the Antarctic Oscillation. The question arises as to what the role of these factors has been over the past decades has been.

All reconstructions show interdecadal variability. The SON index also has positive values around 1960, although these values are not the highest of the series. However, only tentative conclusions can be drawn on the AAOI in SON, because of the low fitting and calibration statistics.

As stated above, in DJ and MAM, there are sufficient stations with long enough records to produce a reconstruction back to 1866 (16 and 11 respectively). Figure 7 shows these reconstructions, together with the 1905 and 1951 reconstructions. The fitting and validation statistics are good in DJ, with a validation correlation of 0.83 and an RE of 0.68. Agreement between the 1866 reconstruction and the other two reconstructions is good, with interannual correlations of 0.86 and 0.84 and low frequency (9 year) correlations of 0.91 and 0.91 with the 1905 and 1951 reconstructions respectively. In MAM the validation statistics are moderately good, the validation correlation is 0.74, and the RE 0.54. The interannual correlations between the 1866 reconstruction are 0.77 and 0.89 with the 1905 and 1951 reconstructions respectively, and the low-frequency correlations are 0.79 and 0.92 with the 1905 and 1951 reconstructions respectively.

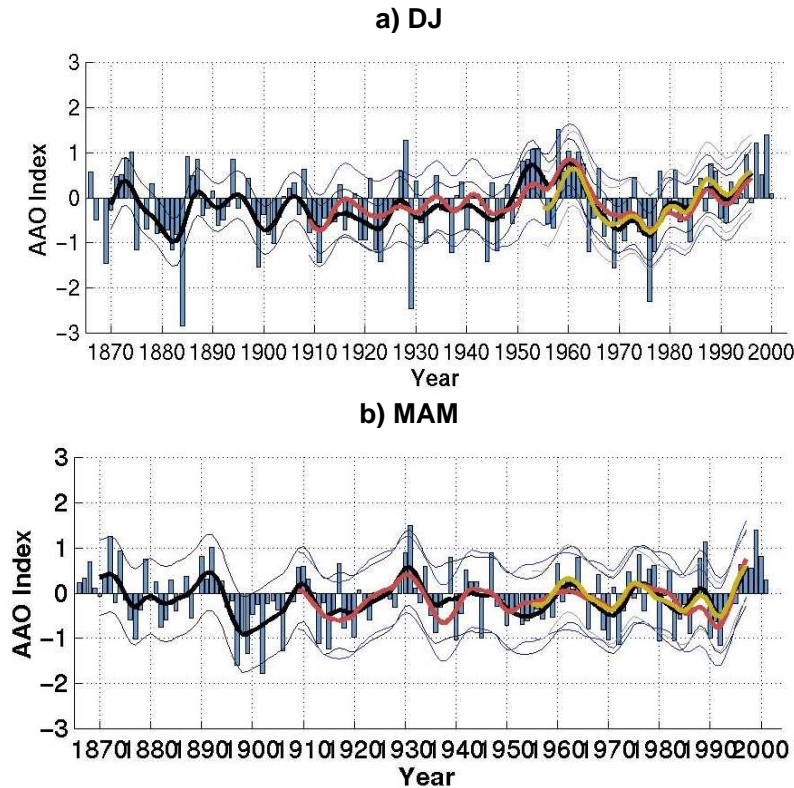


**Figure 7.** The DJ AAO Index reconstructed back to 1866 (blue bars), 9 year filtered reconstruction (thick black line), 9 year filtered 1905 (1951) reconstructions (thick red (yellow) line).

## II.1.2. Pattern Nudging results

As a basis for the presentation of ECHAM4 simulations with pattern nudging, the first subsection reviews the conceptual basis of pattern nudging. The method was invented before the project started and first test simulations were available then. However, it turned out during the early phase of the project that the implementation in ECHAM4 was not yet operational. Several errors in the original implementation were identified and corrected, and many simulations have been run in order to optimise the specific setup. During the project the main pattern nudging module for ECHAM4 as well as the code to produce the input files were completely rewritten, in order to make them less error prone, more flexible, and more user-friendly. The second subsection presents a brief overview of our recent simulations. The definition of input fields for pattern nudging is given in subsection 3. In subsection 4 some results of nudging towards constant circulation anomalies are presented, while in subsection 5 first results of a transient run with nudging towards historic circulation anomalies are shown.

### II.1.2.1. Method Overview

Assimilation of observations in GCMs, for instance from surface stations, balloon soundings, or satellites, has been operationally employed for many years to find the initial conditions needed for numerical weather prediction (NWP), as well as to obtain atmospheric reanalyses. In these cases sophisticated schemes based on Kalman filters and variational techniques, which take into account the estimated covariance structure of the errors in the observations and the simulation (for an overview see Swinbank 2004). Data assimilation in GCMs has also been used for process studies and model validation, usually using the simpler, so-called nudging method, which directly relaxes the model

states towards local observations or large-scale target fields (e.g. Timmreck et al. 1999, Murphy 2000).

The Kalman filter type methods used in NWP are not ideally suited for assimilation of proxy-based circulation estimates for two main reasons. Firstly, circulation variability is to a large extent internally generated and on the time scales relevant for climate reconstructions the model has no skill in simulating this practically random variability. Although a fraction of the decadal and longer scale circulation variability may also be forced (e.g. Shindell et al. 2001), the dynamics of the circulation response to solar or volcanic forcing is rather complex, not fully understood, and appears to be not sufficiently described by GCM without well-resolved stratospheric dynamics and chemistry. Thus no considerable predictive skill for circulation variability can be expected from many GCMs, including ECHO-G. Secondly, the methods used in NWP require a relatively precise knowledge of the target state. However, proxy data are available only from a few locations and typically represent climate signals that are integrated over several months to decades. In addition large uncertainties exist due to the complex relationship between climate and proxy variables, as well as due to non-climatic influences on the proxy records. Thus, in palaeoclimatology the target state towards which the model should be relaxed is only incompletely known.

To overcome these problems the DATUN method (Data Assimilation Through Upscaling and Nudging) was proposed by Von Storch et al. (2000a). DATUN is tailored towards assimilation problems in palaeoclimatology as it uses a nudging rather than a Kalman type technique (i.e. does not assume predictive skill of the model for the nudged variable) and allows to nudge only the large-scale aspects of circulation variability, for which estimates are relatively reliable due to the averaging of information from many locations. As mentioned above, DATUN consists of two steps. The first step is the formulation of upscaling models, which link proxy data or long instrumental records from multiple sites to the intensities of hemispheric or continental-scale temperature or circulation patterns.

The second step is the assimilation of the estimated large-scale patterns into a GCM with the pattern nudging technique. Conceptually pattern nudging is related, but not identical, to the spectral nudging technique used in regional modelling (Von Storch et al. 2000b).

The core of the pattern nudging method is the expansion of a model field  $\Psi(x,t)$  at a given time in a nudged pattern  $\Phi_T$  (the so-called target pattern) and non-nudged patterns  $\Phi_{i=2:\infty}$  according to

$$\Psi(x,t) = \bar{\Psi}(x) + \alpha_T(t)\phi_T(x) + \sum_{i=2}^{\infty} \alpha_i(t)\phi_i(x)$$

and the calculation of the amplitudes (or time expansion coefficients) of the target pattern by projecting the anomalies of the simulated field

$$\Delta\Psi(x,t) = \Psi_{\text{mod}}(x,t) - \bar{\Psi}(x)$$

onto the target pattern. The time expansion coefficients are thus given by

$$\alpha_{\text{mod}}(t) = \frac{(\Delta\Psi(x,t), \Phi_T(x))}{(\Phi_T(x), \Phi_T(x))}$$

The additional nudging term in the prognostic model equations is then defined by

$$R = G (\alpha_T - \alpha_{\text{mod}}(t)) \Phi_T(x)$$

where  $\alpha_T$  is the target amplitude towards which the model state is nudged.  $G$  is a constant that defines the strength of the nudging.

The time step of the ECHAM4 model used in our experiments is 30 minutes. The target amplitudes are defined for every month. Unless the time step is in the middle of the month, two nudging terms are calculated. One is based on climatologies and target fields respect to for the current month and the second based on climatologies and target fields for the month before or after. The final nudging term is determined by interpolating linearly between the two terms with weights determined by how close the time step is to the centres of the two months.

### ***II.1.2.2. Experiment overview***

The pattern nudging experiments have been performed with the ECHAM4 atmosphere GCM (Roeckner et al. 1996) with a T30 horizontal resolution (approx. 3.75° lat. by 3.75° lon. or 400 km lat. by 400 km lon.) and 19 hybrid sigma-pressure levels with the highest at 10 hPa. During the early test experiments it became clear that the definition of simulated anomalies should be changed from being based on NCEP climatologies to being based on ECHAM climatologies, in order to avoid including nudging terms that are merely due to differences in the mean circulation in ECHAM4 and NCEP. Until spring 2005 we have used an implementation of pattern nudging in an existing more general nudging module for the ECHAM model (`mo_nudging.f90`). As the program structure was not optimised for pattern nudging, we have now completed a new module to specifically perform pattern nudging (`mo_patnudg.f90`). With the new module simulations with time-dependent target amplitudes can be conveniently performed. We have also completely changed the structure of the input data for the pattern nudging. All input (target fields, climatologies, target amplitudes) are now provided in standard netCDF format. The programs to produce the input files have been simplified compared to the earlier version. They now use only standard software (Matlab, CDO, NCO) and well-defined interfaces in netCDF format between the different steps.

All experiments have so far been conducted with the uncoupled ECHAM4 and climatological sea surface temperatures, in order to save computing time during the test phase for pattern nudging. The new nudging module has been successfully compiled with the coupled ECHO-G model and we do not expect any additional technical problems with coupled experiments which are scheduled to start in late 2005/early 2006.

The experiments performed during the project include many simulations with nudging towards various constant target values of the AOI with various nudging constants  $G$ , as well as a recently completed transient experiment in which the model state is nudged towards the actual AOI for the period 1948-2002, which was derived from the NCEP/NCAR reanalysis. The non-transient experiments have been used to gain experience with the pattern nudging and test the response of the model under simple conditions. These simulations were partly described in earlier reports and grey publications (Widmann et al. 2004) and are currently being written up for publication in *Climate Dynamics* (Widmann et al. 2005). The transient experiment represents the final design of the pattern nudging simulations. The analysis of this simulation is in an early stage and comprehensive analysis is on the way. After this we will perform coupled simulations starting at around 1850, which will not pose any new technical or conceptual problems with respect to the pattern nudging.

### ***II.1.2.3. Experiment design and definition of target fields***

In our experiments we want to nudge the NH extratropical atmosphere towards anomalies that are related to AO variability. The primary definition of the AO is as EOF1 of extratropical SLP, but the AO has a well-defined circulation and temperature structure throughout the troposphere (Thompson and Wallace 2000). All prognostic variables can in principle be nudged. In ECHAM4 these are SLP, horizontal vorticity and divergence of the wind field, and temperature. Thus one could attempt to nudge the model towards prescribed AO states either through nudging SLP, or through nudging the wind field or temperature on various vertical levels, or through a combination of these approaches. We decided not to nudge temperature, because the AO is primarily a circulation phenomenon, which affects temperature through advection. We also did not nudge SLP for several reasons. If only SLP

was nudged, most circulation-related variables would still be free, and internally generated variability may make it difficult to keep the atmosphere close to the target state. If circulation in the free troposphere was nudged together with SLP, particular care may be needed to ensure consistency of nudging two different variables and, as SLP would be involved, of conserving the total mass. We decided to keep things as simple as possible and only nudged the circulation.

The nudging is used in the lower and middle troposphere. It is applied to the horizontal vorticity of the wind field, because the wind field in the free, extratropical atmosphere is approximately geostrophic and divergence-free. It will be shown later in this section through a linear analysis of the link between the AO signal in SLP and in the circulation in the free troposphere that one can indeed expect to closely control the SLP AO state by prescribing the circulation in the free troposphere.

We will now describe how the vorticity target patterns for the pattern nudging simulations are specified. We use different patterns for each month of the year, but for brevity present only those for January, April, July, and October. All target patterns have been derived from the NCEP/NCAR reanalysis (Kalnay et al. 1996, Kistler et al. 2001). Following the standard AO definition, we start with calculating the AO pattern for each month of the year as EOF1 of detrended SLP between 20°N and 85°N for the period 1948 - 2002 (Figure 8, for brevity only four months are shown). The AOI is then calculated by projecting the non-detrended, monthly SLP anomalies (with respect to the 1948-2002 mean for a given month of the year) onto the AO pattern. This projection includes area weighting to account for the different areas represented by the regular latitude-longitude grid on which the SLP data are given.

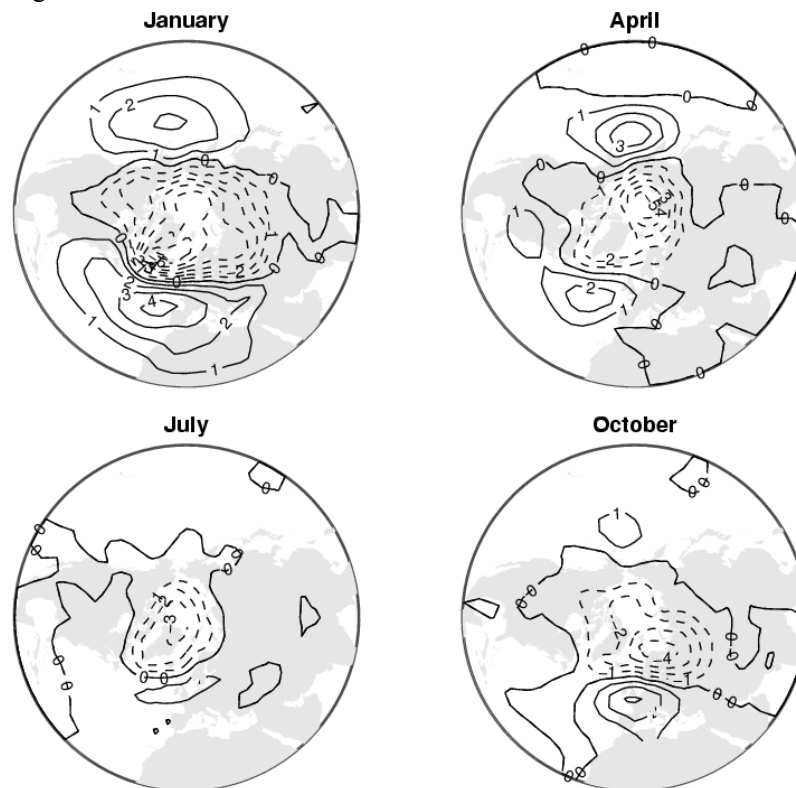


**Figure 8.** First EOFs of NH extratropical, detrended, monthly NCEP SLP for the period 1948-2002. Shown are the pressure anomalies in hPa associated with a value of PC1 of one standard deviation.

The vorticity target patterns are defined as the linear signal of the AOI in the horizontal vorticity of the NCEP/NCAR wind field. They are determined by regressing the horizontal vorticity onto the AOI. These patterns are directly used in the pattern nudging simulations, and therefore need to be

defined on the ECHAM4 model grid and on the model levels. For this purpose we first derive for each month of the year the mean pressure on the 19 model levels from 20 years of an ECHO-G equilibrium simulation. We use the coupled model to define the climatological model levels, because the final application of pattern nudging will also use the coupled model. The  $u$  and  $v$  components of the NCEP/NCAR reanalysis wind field are then interpolated from the 2.5 deg reanalysis grid onto the ECHAM grid and from pressure levels onto the climatological model levels. Finally the horizontal vorticity for the period 1948-2002 is calculated from the wind field on the ECHAM4 grid and model levels and regressed onto the AOI separately for each month of the year and each level. The regression is restricted to the domain  $20^{\circ}\text{N}$  and  $85^{\circ}\text{N}$ , outside the vorticity target patterns are set to zero.

The model is nudged on levels 10 to 16. The maximum pressure (with respect to space) of the climatological mean on these levels ranges from 424 hPa (level 10) to 980 hPa (level 16). The differences between the month of the year are only about 2 hPa. Lower levels are excluded to avoid the layer with the strongest ageostrophic components and boundary effects that may be difficult to simulate. Higher levels are excluded because the relationship between the AAOI and the wind field can be expected to be strongest for the lower troposphere. As an example, the regression maps on level 14, on which the maximal mean pressure is 825 hPa, are shown in (Figure 9). They contains relatively small structures, which can be expected because the vorticity field is the Laplacian of the SLP field.

regression coeff., model level 14, monthly rel. vort. and monthly AO index

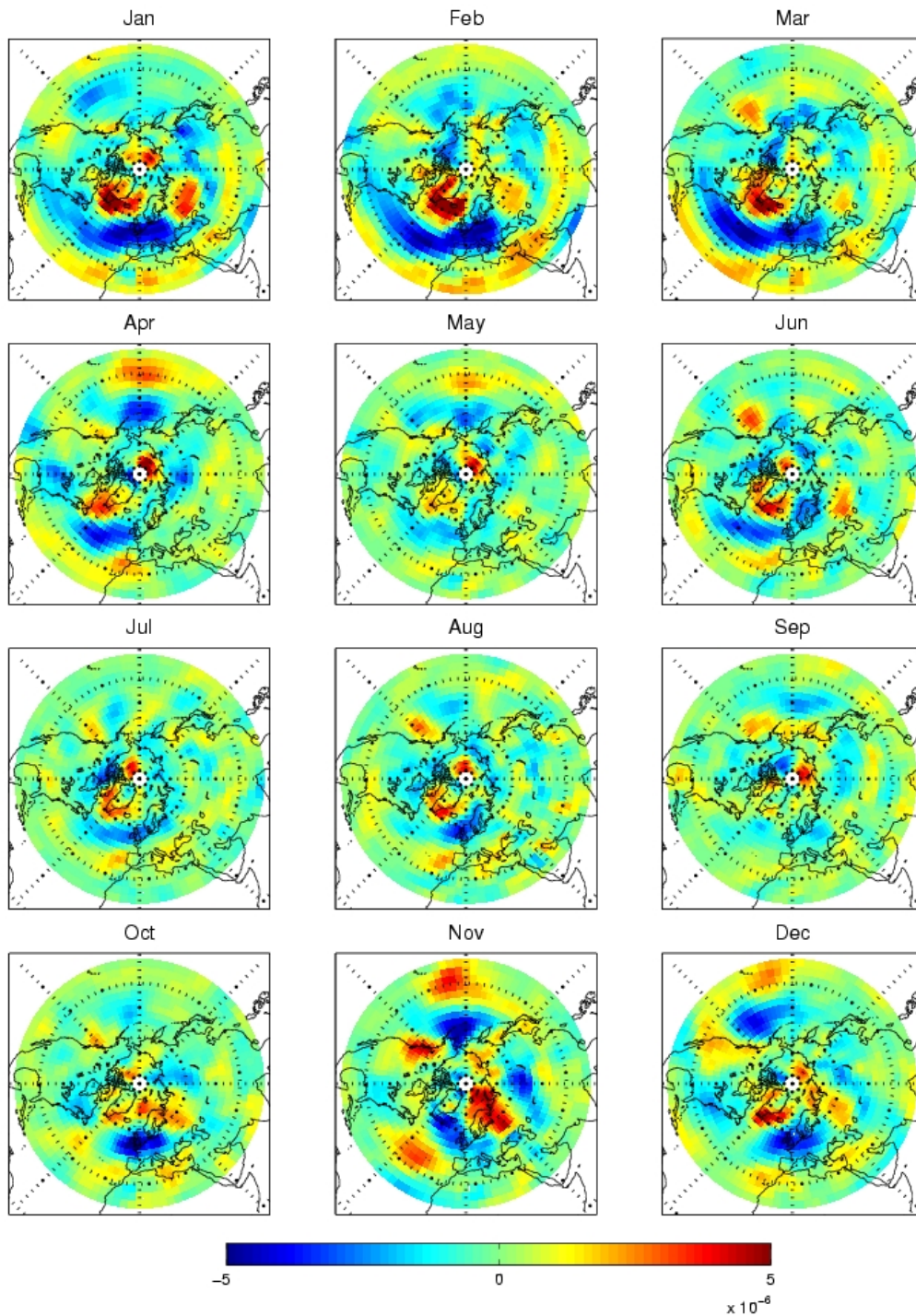


**Figure 9.** Regression coefficients of monthly means of relative horizontal vorticity regressed on monthly AO indices 1948 - 2002. The map shows the vorticity change in  $10^{-6} \text{ s}^{-1}$  associated with a positive change of the AO index of one standard deviation.

The definition of the vorticity target pattern by regressing the vorticity field onto the AOI is intuitively an obvious choice. However it is not immediately obvious how to describe the strength of the linear connection between the AOI and the regression map. If we estimate the AOI by multiple linear regression (MLR) from the vorticity field, we can use the coefficient of determination to describe the

strength of the coupling, but the regression weights may not be proportional to the regression map. If we chose an ad hoc approach and calculate the correlation between the time expansion coefficient (TEC) of the regression map and the AOI the meaning of the former is not entirely clear. This problem led to a systematic analysis of the relation between regression maps and one-dimensional Canonical Correlation Analysis (CCA) and Singular Value Decomposition (SVD), which is published in *J. Climate* (Widmann 2005). It was shown that regression maps are identical to signals of a time series in a spatial field independently of whether local regressions, CCA or SVD are used. If the time series is linearly estimated from the spatial field, the regression map is proportional to the weights obtained by the SVD model, but different to the weights obtained from CCA and MLR. The application to our problem is that calculating the correlation between the time expansion coefficient of the regression map and the AOI is conceptually well defined and equivalent to applying an SVD model.

We thus express the strength of the linear relation between the AOI and the vorticity regression maps through the correlation of AOI and the TEC of the vorticity regression map. The latter is calculated by projecting the vorticity anomalies for a given month and level onto the regression map (with proper area weighting). The correlations range from 0.94 in February and for TECs on level 16 to 0.76 in September and for TECs on level 10. In all months the correlations tend to decrease slightly with height. These high correlations show that there is a close linear relationship between the AOI and the TECs of the vorticity maps.

In our pattern nudging experiments the vorticity regression maps are prescribed as anomalies in the vorticity field and thus the question arises what SLP anomalies are most closely linearly related to these vorticity regression maps, and whether these SLP anomalies have the structure of the AO. Despite the high correlations between the AOI and the TECs of the vorticity maps, there are no theoretical arguments that ensure an AO structure of the linear SLP signal of the TECs of the vorticity maps. For the real world, we can determine this SLP signal from reanalysis data by regressing the SLP field onto the TECs of the vorticity regression maps. An example using SLP from the reanalysis and TECs on level 14 is shown in Fig 10. These regression maps are almost identical to the AO patterns shown in Fig. 8. The same is true for all other months and TECs from other levels and the reanalysis data thus suggest that it may indeed be possible to obtain an AO anomaly in the SLP field by prescribing the wind field in the lower and middle troposphere. To what extent this finding applies to the ECHAM4 model world will be investigated through an analogous analysis later in this report.

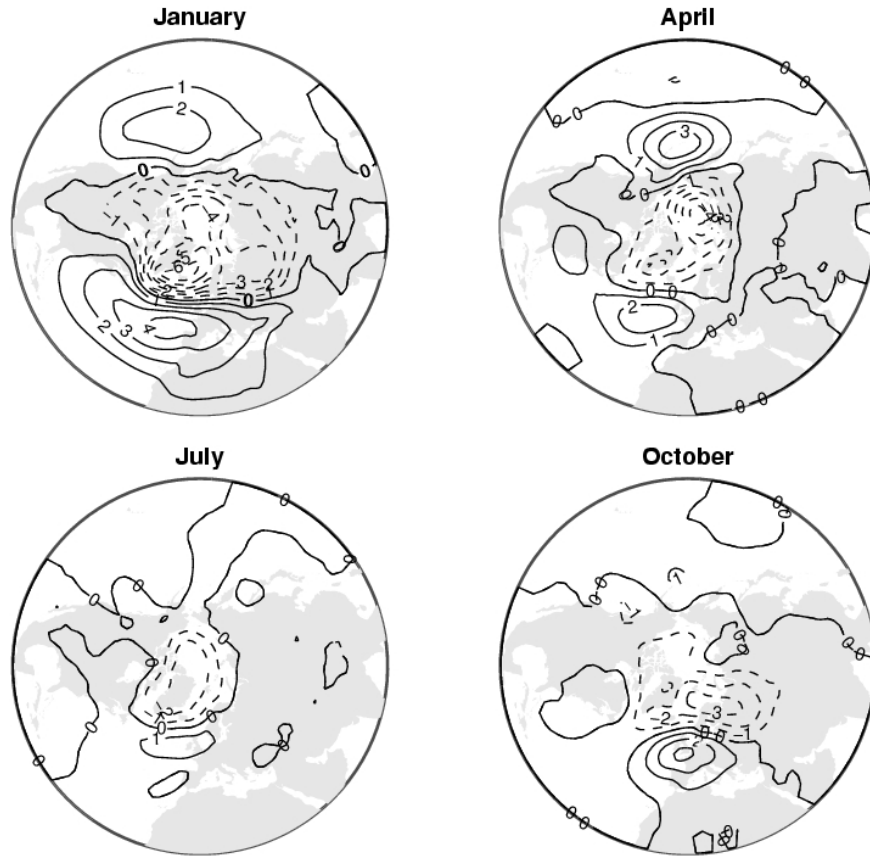


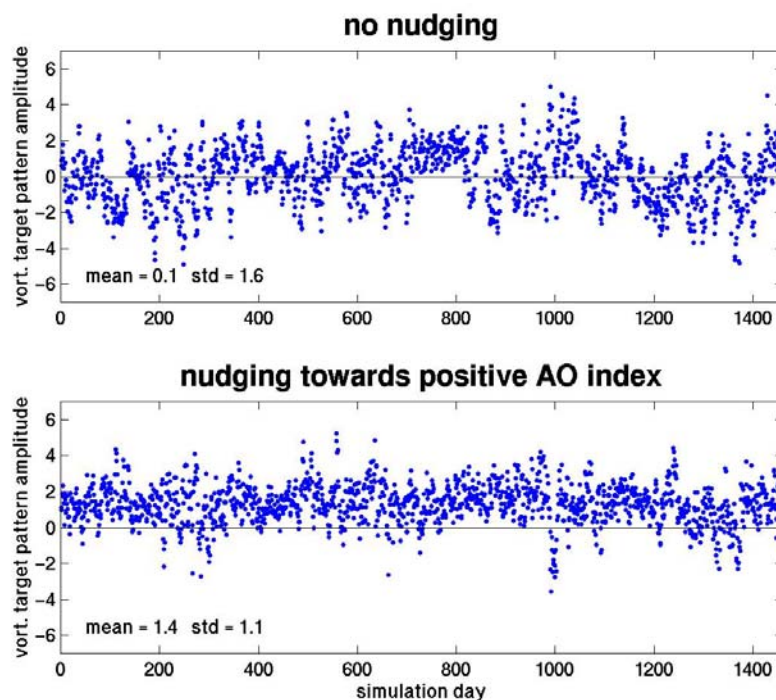
**Figure 10.** Regression coefficients of monthly NCEP/NCAR reanalysis SLP from 1948 - 2002 regressed on the time expansion coefficient of reanalysis vorticity regression maps interpolated on ECHAM model level 14. Shown are the pressure anomalies in hPa associated with a positive change of the time expansion coefficient of one standard deviation.

In order to determine the nudging terms, the TECs of the vorticity target pattern need to be calculated for a given model state by projecting the simulated vorticity anomaly onto the target pattern. The vorticity climatologies with respect to which the anomalies are calculated could be taken from the real world, for instance from the NCEP/NCAR reanalysis, or from the ECHAM model. If the climatologies were based on real world data, differences between the mean circulation in the model and the real circulation would affect the TEC and the nudging terms (provided the difference is not orthogonal to the target pattern). The mean climate of a control simulation without nudging would not have a mean TEC of the vorticity target pattern of zero, which would make a comparison between nudged and free simulations difficult. We therefore defined the climatologies as the mean horizontal vorticity of a 30 year long free ECHAM4 simulation. Thus nudging towards a specific non-zero target TEC of the target pattern will nudge the simulated states away from the mean state in the model.

#### ***II.1.2.4. Results of nudging towards constant target amplitudes***

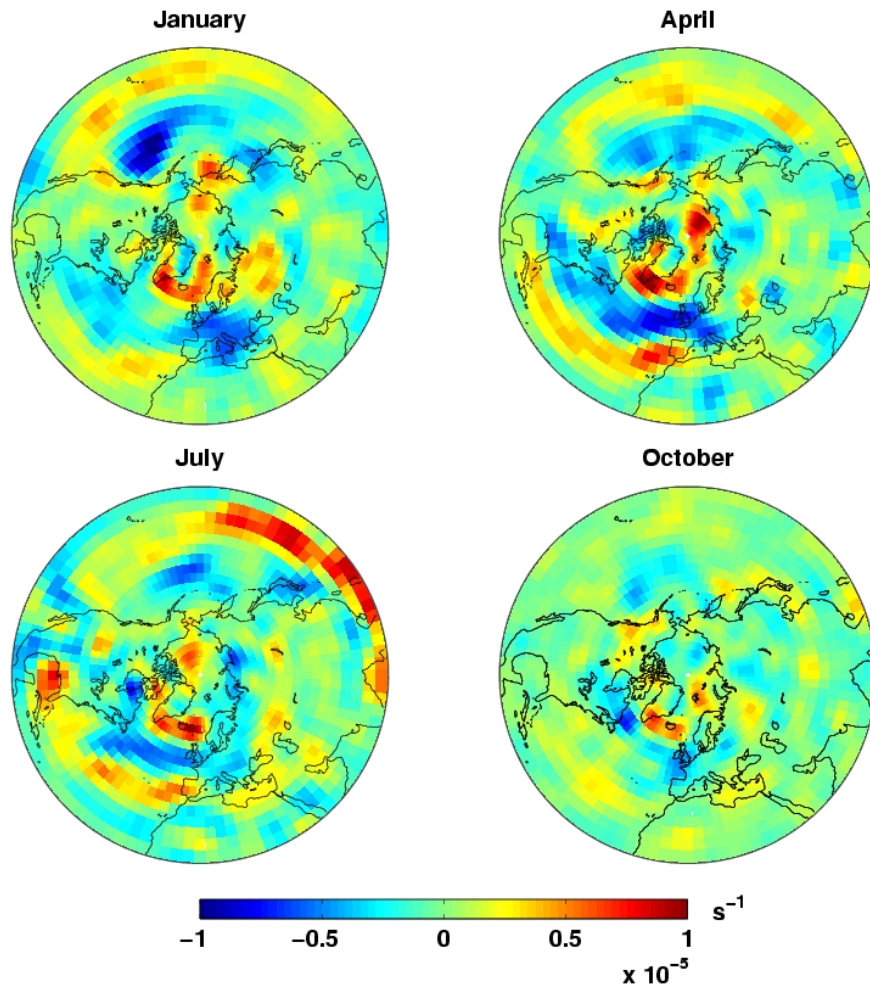
In this section the response of ECHAM4 to nudging towards a constant AOI is discussed. We have performed several simulations with lengths between 5 and 20 years in which the target amplitude of the vorticity target pattern was set constant during the simulations. The target amplitudes in the different simulations represented AO indices between  $-2$  and  $2$  standard deviations and relaxation times were varied between 12 hours (h) and 5 days. We have also performed a 30 year long control run in which the nudging was switched off, but the TECs of the target patterns were still calculated.

Fig. 11 shows an example for daily TECs of the vorticity target pattern on level 14 for the first 4 years of the control simulation and of a 20 year long simulation in which we nudged towards a target amplitude of 2 with a nudging constant  $G$  that is equivalent to an relaxation e-folding time of 2 days. With this setting it is possible to obtain a mean TEC of the vorticity pattern that is significantly positive and still retain considerable variability in the TEC. The latter property is desirable for applications in palaeoclimatology where only seasonal or longer-scale means of circulation anomalies can be estimated. The bias between target amplitude of 2 and the mean TEC of 1.4 (with respect to the entire 20 year simulation period) could be taken into account by nudging towards higher target values that could be derived from an objectively determined response function. Alternatively, one can use somewhat stronger nudging terms with relaxation times around 1 day, which, as will be shown later, produces almost bias-free simulations but reduces the variability somewhat stronger. We intend to use relaxation times of 1 day in applications where the target values are well known on an approximately monthly-seasonal time scale, which is typically the case for instrumental-based estimates, and relaxation times of 2 days or longer for nudging towards estimates from proxy data.



**Figure 11.** Daily TECs of the vorticity target pattern on level 14 for the first 4 years of a control simulation (upper panel) and in a simulation with nudging towards a target amplitude of 2 with a relaxation time of 2 days.

The response of the model in the vorticity field on level 14 (around 825 hPa) is displayed in Fig. 12, which shows the mean difference in relative vorticity between the aforementioned 20 year long simulation nudged towards an AOI of 2 with a relaxation time of 2 days and the 30 year long control simulation (for brevity only 4 months are shown). A comparison with Fig. 9 shows that the mean difference is very similar to the target patterns. It should be noted that this does not necessarily have to be the case, because the amplitudes of patterns orthogonal to the target pattern, which are not nudged, could be dynamically linked to the target pattern. At least for the vorticity signal of the AO this seems not to be the case, and the response of the model towards the pattern nudging is quite direct and the pattern nudging of vorticity is successful not only in terms of the amplitude of the target anomaly, but also in terms of the spatial structure of the model response. Note also that the colour bars differ by a factor of two, reflecting that Fig.9 represents the vorticity signal of an AO change of one standard deviation, while the response patterns in Fig. 11 have amplitudes of around 1.4.



**Figure 12.** Vorticity response of ECHAM4 to pattern nudging. The figure shows the mean difference in relative vorticity on model level 14 (around 825 hPa) between the a 20 year long simulation nudged towards an AOI of 2 with a relaxation time of 2 days and a 30 year long control simulation.

The next question is whether the response to pattern nudging in the vorticity field is associated with an AO-type response in the SLP field. The SLP difference between the same simulations that were used for Figs. 11 and 12 is shown in Fig. 13. In January, April and October the difference clearly resembles the AO-patterns shown in Fig. 8, with negative SLP anomalies over the pole and increased pressure over the mid-latitudes. The zero-line of the difference is very close to the one in AO pattern, the amplitudes are consistent with the AOI of around 1.4 that is reached with the nudging, but the individual centres of action in Fig. 13 and Fig. 8 differ somewhat in location and amplitude (taking into account that the response is for an AOI of 1.4). In July the response pattern is considerably different from the AO-pattern, as the former shows pronounced positive anomalies over the Atlantic and the Pacific and negative anomalies in low latitudes, which both are not part of the AO-pattern.

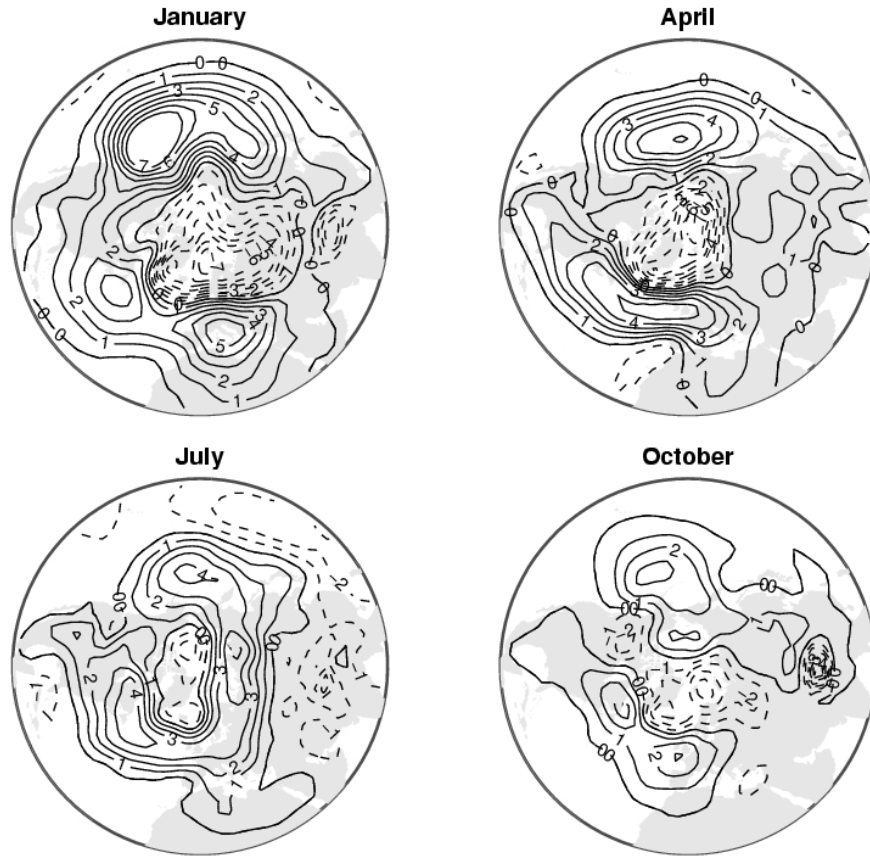


**Figure 13.** SLP difference in hPa between the same simulations that were used for Figs. 11 and 12

There may be several reasons for the difference between the two sets of patterns. Firstly EOFs are statistical constructs and do usually not represent actual anomalies in certain situations. Roughly speaking the AO pattern rather shows the average structure of anomalies in situations where the AO index is particularly high or low. We do not necessarily expect the SLP in positive AOI situations to look exactly like EOF1. Secondly the structure of SLP variability in ECHAM4 may be different from the real world. Thirdly the relation between the vorticity and the SLP field may be different in the model and in reality. Yet, one would still expect SLP responses that roughly agree with the AO-pattern. Thus the differences between mean SLP response to pattern nudging and the AO-pattern in January, April, and October may well be within acceptable limits, whereas the response in July indicates difficulties with nudging towards specified AOI situations in summer. The latter may be partly attributable to the fact that the AO is less pronounced in summer, i.e. explains a smaller fraction of the SLP variability.

To find out more about the reason for the differences we have analysed the structure of circulation variability in the ECHAM4 control simulation. Analogous to Fig. 8, which is based on the NCEP reanalysis, we have calculated SLP EOF1 in ECHAM4 (Fig. 14), and analogous to Fig. 10 we have regressed the ECHAM4 SLP field on the amplitudes of the vorticity target patterns (Fig. 15). These amplitudes were calculated by projecting the vorticity anomalies of the ECHAM4 control simulation onto the target patterns which were defined as above. A comparison of the real-world and simulated AO-patterns (Figs. 8 and 14) shows that the AO in ECHAM4 has in general the right structure and amplitude, but there are also noticeable differences, most prominently the smaller extension and eastward shift of the January Atlantic centre of action, and extension of the October polar negative anomaly over Alaska. We have also looked at SLP EOFs from other ECHAM4 simulations and found evidence of some sampling variability. Nevertheless, we can conclude that the SLP response patterns

are not closer to ECHAM4 EOF1 than to the NCEP EOF1. Note that this is true also for July, where the differences between the response pattern and the NCEP EOF1 was largest. The ECHAM4-based regression maps in Fig.15 are similar to the EOFs from ECHAM4 and from NCEP. Where the ECHAM4 and NCEP EOFs differ, the structure of the regression map is in general more similar to the NCEP pattern, for instance with respect to the location and extension of the January Atlantic centre of action, and to the October positive centre west of Alaska. In summary this suggests that the difference between SLP response pattern and SLP EOFs is not mainly attributable to differences between model and reality in the circulation variability. In autumn, winter, and spring it seems more a consequence of the fact that EOFs and regression maps are statistical idealisation, which do not exactly represent actual anomalies. The difference in summer seems too big to be explained in this way, but we have not found yet alternative explanations.

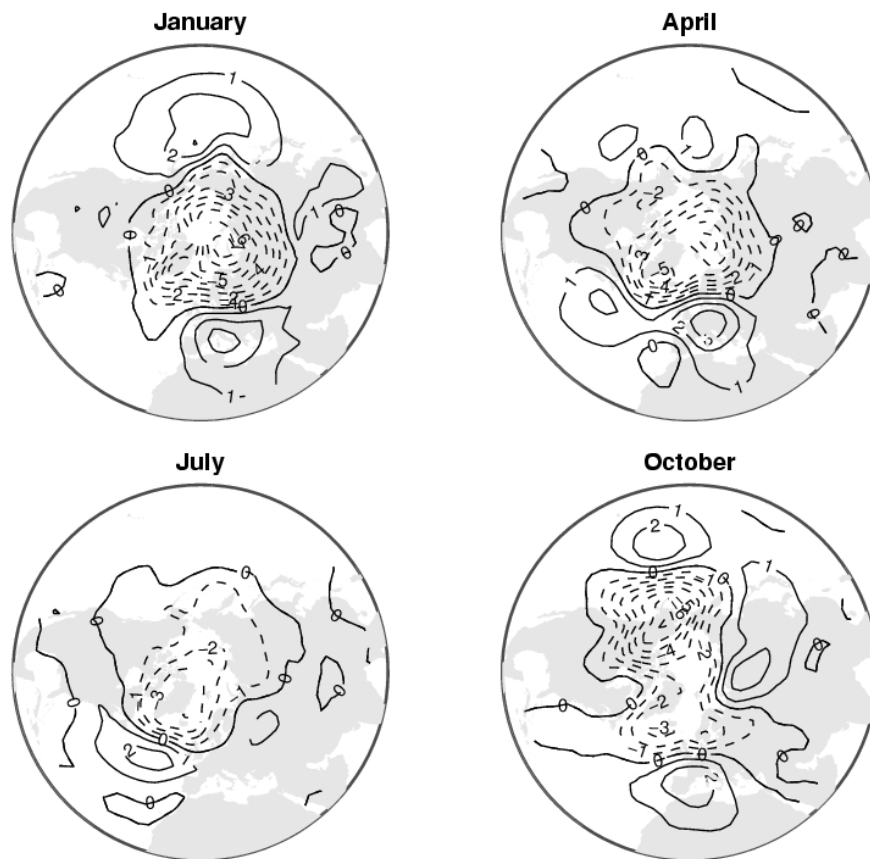


**Figure 14.** SLP EOF1 derived from a non-nudged ECHAM4 simulation.

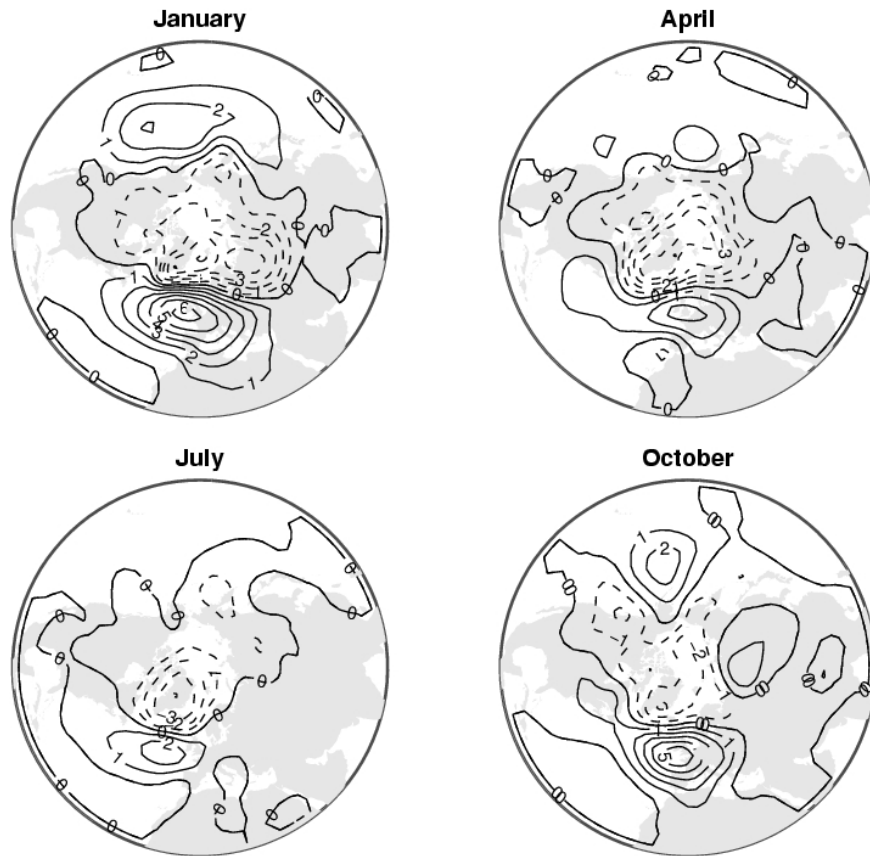


**Figure 15.** Regression coefficients of monthly SLP anomalies from a non-nudged ECHAM4 simulation regressed on the time expansion coefficient of reanalysis vorticity regression maps on ECHAM model level 14. Shown are the pressure anomalies in hPa associated with a positive change of the time expansion coefficient of one standard deviation.

So far only the mean response of ECHAM4 to pattern nudging was discussed. A pivotal aspect of pattern nudging, which distinguishes it from existing grid-point-based or full-field nudging methods is that it is designed to allow prescribing large-scale circulation anomalies without suppressing variability of non-nudged circulation properties. In order to test whether this is actually achieved, we have calculated the synoptic-scale variability in the control and in nudged simulations. Fig. 15 shows the 2-6 day bandpass-filtered variability of 500 hPa geopotential height for the control simulation and for the nudged simulation on which the previous figures were based. It shows that the total variability is not reduced in the nudged simulation and that the stormtracks respond in a physically plausible way to the nudging towards a positive AOI by extending further into northern Europe and western Canada.

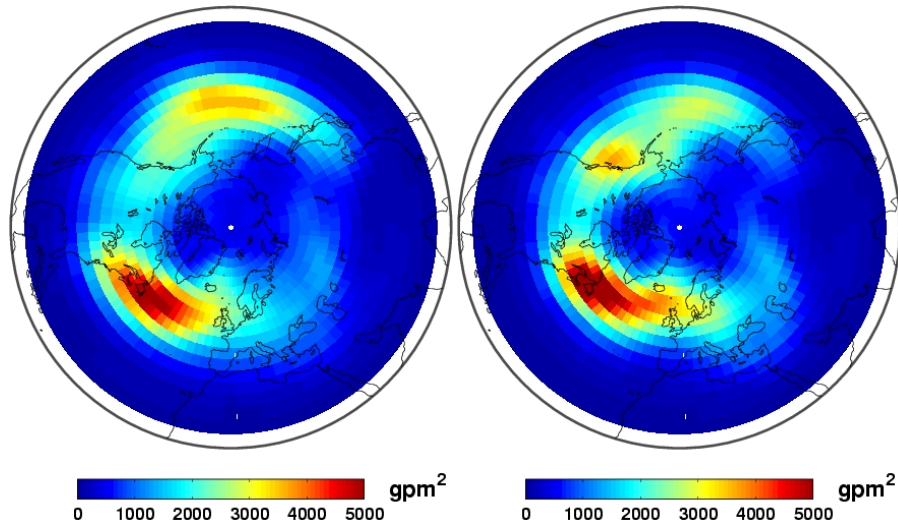


**Figure 16.** 2-6 day bandpass-filtered variability of 500 hPa geopotential height for the control simulation and for the nudged simulation presented in Figures 11-13.

#### *II.1.2.5. Pattern nudging towards transient target amplitudes*

We have recently completed a simulation with the new pattern nudging module `mo_patnudg.f90` for the period 1948-2002 in which ECHAM4 was nudged towards the monthly AO indices derived from the NCEP reanalysis. We have used a relaxation time of 1 day, because the target values have a high accuracy. The analysis of this first transient simulation with pattern has just started. Fig. 17 shows the NCEP AOI together with monthly means of the amplitude of the vorticity target pattern on ECHAM level 14. This amplitude follows the NCEP AOI closely and thus shows that the pattern nudging techniques is well suited for transient simulations. A comprehensive comparison of this simulation with the NCEP reanalysis will follow in order to investigate which aspects of the climate variability can be captured when the AOI is prescribed with pattern nudging.

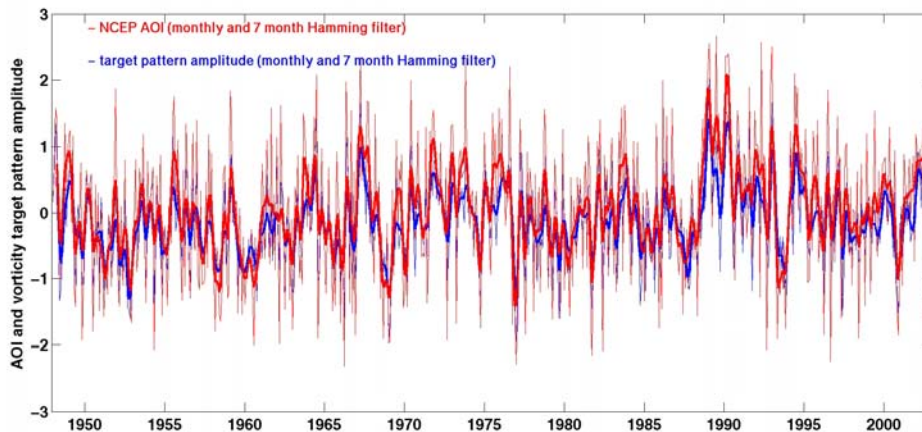


**Figure 17.** Monthly and filtered AO Index from the NCEP reanalysis and time expansion coefficient of the AO vorticity signal in an ECHAM4 simulation with pattern nudging.

## **II.2. Voraussichtlicher Nutzen, insbesondere der Verwertbarkeit des Ergebnisses im Sinne des fortgeschriebenen Verwertungsplans**

The AOI reconstructions provide for the early period of gridded data an alternative and internally consistent approach to calculating the AOI directly as PC1 of the gridded data. The two approaches can be compared to estimate the uncertainties in the AOI estimates. The AAO reconstructions are useful both as input to the data assimilation, but also in their own right. As explained above, in the SH, little is known about large-scale circulation prior to the period when reanalysis data is available (1948/1958).

The pattern nudging assimilation method that has been tested and optimised during the project will allow for the first time GCM simulations for the past climate that take into account empirical estimates for circulation variability. These have the potential to be more realistic than standard transient simulations without assimilation, because circulation variability is partly internally generated and random and therefore not captured without assimilation, and partly linked to forcings through processes that are difficult to simulate.

## **II.3. Während der Durchführung des Vorhabens dem ZE bekannt gewordener Fortschritt auf dem Gebiet des Vorhabens bei anderen Stellen**

Data assimilation for applications in paleoclimatology has been undertaken with an intermediate complexity model by Schrier and Bargtmeijer (2005). These authors performed non-transient simulations for prescribed idealised atmospheric states by using an adjoint method. This approach is not applicable to long GCM simulations, as the adjoint of the tangent linear operator of the dynamical system needs to be calculated at every time step, which is not affordable for long simulations with full complexity models.

A global gridded SLP dataset back to 1850 is currently in preparation by Rob Allan and Tara Ansell from the Hadley Centre (UK) (Allan and Ansell 2005), and a beta version has been made available to the authors. This will allow comparison with both the reconstructions, and the transient assimilated simulation. This dataset shall not be used to define the indices and patterns for assimilation, as during the early period of the dataset, particularly in the SH, interpolation of stations over large distances has been undertaken. Thus during the early period, this dataset cannot be regarded as the true AAOI.

Progress has also been made on multiproxy reconstruction of European circulation and SLP during the running time of the project, for example of the NAO index (Timm et al. 2004, Cook et al. 2002), the AO index (D'Arrigo et al. 2003), and SLP over the Eastern North Atlantic from early instrumental and documentary data Europe (Luterbacher et al. 2002). Schmutz et al. (2001) have reconstructed 700, 500 and 300 hPa geopotential height over the Europe and eastern North Atlantic region for 1901-1947 using SLP, temperature and precipitation. Bronnimann and Luterbacher (2004) and Bronnimann et al. (2004) have reconstructed upper-level temperature and geopotential height fields for the NH during World War II, using meteorological measurements. These non proxy-based reconstructions will be useful for evaluation of the assimilation run.

## **II.4. Erfolgte oder geplante Veröffentlichung des Ergebnisses nach Nr. 11**

### ***published***

Jones, J. M. and M. Widmann, 2004. Early peak in Antarctic Oscillation index. *Nature*, **432**, 290-291.

Widmann, M., J. M. Jones and H. von Storch, 2004. Reconstruction of large-scale atmospheric circulation and data assimilation in paleoclimatology. *Pages Newsletter*, **12(2)**, 12-13.

Widmann, M. One-dimensional CCA and SVD and their relationship to regression maps. *J. Climate*, **18(14)**, 2785-2792

*in preparation*

Jones, J. M. Seasonal reconstructions of the Antarctic Oscillation.

Widmann, M., H. von Storch, R. Schnur, and I. Kirchner. Assimilation of large-scale circulation states into the ECHAM 4 atmospheric GCM with Pattern Nudging.

## References

Allan, R. J., and T. J. Ansell, 2005. A new globally complete monthly historical gridded mean sea level pressure data set (HadSLP2): 1850-2003. *In preparation*.

Briffa, K R, T. J. Osborn, F. H. Schweingruber, I. C. Harris, P. D. Jones, S. G. Shiyatov, and E. A. Vaganov, 2001: Low-frequency temperature variations from a northern tree ring density network. *J. Geophys. Res.*, **106**, 2929-2941.

Basnett, T. and Parker, D., 1997. Development of the Global Mean Sea Level Pressure Data Set GMSLP2, Climate Research Technical Note, 79, Hadley Centre, Met Office, Fitzroy Rd., Exeter, Devon, EX1 3PB, UK.

Bromwich, D. H. and R. L. Fogt, 2004. Strong trends in the skill of the ERA40 and NCEP-NCAR reanalyses in the High and Midlatitudes of the Southern Hemisphere, 1958-2001. *J. Climate*, **17**, 4603-4619.

Bronnimann, S., J. Luterbacher, J. Staehelin, T. M. Svendby, G. Hansen, and T. Svenoe, 2004. Extreme climate of the global troposphere and stratosphere in 1940-42 related to El Nino. *Nature*, **431**, 971-974.

Bronnimann, S. and Luterbacher, J., 2004. Reconstructing Northern Hemisphere upper-level fields during World War II. *Clim. Dyn.*, **22**, 499-510.

Chen, T., and M. Yen, 1997. Interdecadal variation of the Southern Hemisphere circulation. *J. Climate*, **10**, 805-812.

Cook, E., R. D'Arrigo and M. E. Mann, 2002. A well-verified, multiproxy reconstruction of the winter North Atlantic Oscillation index since A.D. 1400. *J. Clim.*, **15**, 1754-64.

Cullen, H, R D D'Arrigo, E R Cook, and M E Mann, 2001: Multiproxy-based reconstructions of the North Atlantic Oscillation over the past three centuries. *Paleoceanography*, **16**, 27-39.

D'Arrigo, R.D., E. R. Cook, M. E. Mann, and G. C. Jacoby, 2003. Tree-ring reconstructions of temperature and sea-level pressure variability associated with the warm-season Arctic Oscillation since AD1650. *Geophys. Res. Lett.*, **30**, art. No. 1549.

Fritts, H C, T J Blasing, B P Hayden, and J E Kutzbach, 1971: Multivariate techniques for specifying tree-growth and climate relationships and for reconstructing anomalies in paleoclimate. *J. Appl. Meteor.*, **10**, 845-864.

- Gillett, N. P and D. W. J. Thompson, 2003. Simulation of recent Southern Hemisphere climate change. *Science*, **302**, 273-275.
- Jones, J. M. and M. Widmann, 2004a: Reconstructing large-scale variability from palaeoclimatic evidence by means of Data Assimilation Through Upscaling and Nudging (DATUN). In: *The KIHZ project: towards a synthesis of Holocene proxy data and climate models*. Springer, Heidelberg, Berlin, New York. ISSN 1437-028X
- Jones, J. M. and M. Widmann, 2004b. Early peak in Antarctic oscillation index. *Nature*, **432**, 290-291.
- Jones, J. M., and M. Widmann, 2003. Instrument- and tree-ring-based estimates of the Antarctic Oscillation. *J. Climate*, **16**, 3511-3524.
- Jones, J.M. and T. D. Davies, 2000. The influence of climate on air and precipitation chemistry over Europe and downscaling applications to future acidic deposition, *Climate Research*, **14**, 7-24.
- Jones, P. D., 1991. Southern Hemisphere sea-level pressure data: an analysis and reconstructions back to 1951 and 1911, *Int. J. Climatol.*, **11**, 585-607.
- Jones, P. D., K. R. Briffa, T. P. Barnett, and S. F. B. Tett, 1998. High-resolution palaeoclimatic records for the last millennium: interpretation, integration and comparison with General Circulation Model control-run temperatures. *Holocene*, **8**, 455-471.
- Jones, P. D., et al. 1999a. Monthly mean pressure reconstructions for Europe for the 1780-1995 period. *Int. J. Climatol.*, **19**, 347-364.
- Jones P. D., M. J. Salinger and A. B. Mullan, 1999b. Extratropical circulation indices in the Southern Hemisphere based on station data. *Int. J. Climatol.*, **19**, 1301-1317.
- Kalnay, E., M. Kanamitsu, R. Kistler, W. Collins, D. Deaven, L. Handin, M. Iredell, S. Saha, G. White, J., Woollen, Y. Zhu, M. Chelliah, W. Ebisuzaki, W. Higgins, J. Janowiak, K. C. Mo, C. Ropelewski, J. Wang, A. Leetmaa, R. Reynolds, R. Jenne, and D. Joseph, 1996: The NCEP-NCAR 40-year reanalysis. *Bul. Amer. Meteor. Soc.*, **77**, 437-471.
- Kistler, R., E. Kalnay, W. Collins, S. Saha, G. White, J. Woollen, M. Chelliah, W. Ebisuzake, M. Kanamitsu, V. Kousky, H. van den Dool, R. Jenne, and M. Fiorino, 2001: The NCEP-NCAR 50-year reanalysis: Monthly means CD-ROM and documentation. *Bull. Amer. Meteor. Soc.*, **82**, 247-267.
- Kushner, P. J., I. M. Held, and T. L. Delworth, 2001. Southern Hemisphere atmospheric circulation response to global warming. *J. Climate*, **14**, 2238-2249.
- Legutke, S. and R. Voss, 1999. The Hamburg atmosphere-ocean coupled circulation model ECHO-G. Technical Report no. 18, German Climate Computing Center (DKRZ), Hamburg.
- Luterbacher, J., E. Xoplaki, D. Dietrich, R. Rickli, J. Jacobeit, C. Beck, D. Gyalistras, C. Schmutz, and H. Wanner, 2002. Reconstruction of sea level pressure fields over the eastern North Atlantic and Europe back to 1500. *Clim. Dyn.*, **18**, 545-561.
- Luterbacher, J. et al. 2000. Monthly mean pressure reconstruction for the late maunder minimum period (AD1675-1715). *Int. J. Climatol.*, **20**, 1049-1066.
- Luterbacher, J. C. Schmutz, D. Gyalistras, E. Xoplaki, and H. Wanner. 1999. Reconstruction of monthly NAO and EU indices back to AD 1675. *Geophys. Res. Lett.*, **26**, 2745-2748.

- Mann, M. E., R. S. Bradley, and M. K. Hughes, 1998: Global-scale temperature patterns and climate forcing over the past six centuries. *Nature*, **392**, 779-787.
- Mann, M. E., R. S. Bradley, and M. K. Hughes, 1999: Northern hemisphere temperatures during the past millennium. *Geophys. Res. Lett.*, **26**, 759-762.
- Mann, M.E., R. S. Bradley and M. K. Hughes. 2000. Long-term variability in the El Nino Southern Oscillation and associated teleconnections, Diaz, H.F. & Markgraf, V. (eds) *El*
- Marshall, G. J., 2003. Trends in the Southern Annular Mode from Observations and Reanalyses. *J. Clim.* **16**, 4134-4143.
- Murphy, J., 2000. Predictions of climate change over Europe using statistical and dynamical downscaling techniques. *Int. J. Climatol.*, **12**, 489-501.
- Rauthe, M., A. Hense, and H. Paeth, 2004. A model intercomparison study of climate change-signals in extratropical circulation. *Int. J. Climatol.*, **24**, 643-662.
- Rind, D., J. Perlwitz, and P. Lonergan, 2005a. AO/NAO response to climate change: 1. Respective influences of stratospheric and tropospheric climate changes. *JGR atmospheres*, **110 (D12)**, Art. No. D12107
- Rind D, J. Perlwitz, P. Lonergan and J. Lerner, 2005b. AO/NAO response to climate change: 2. Relative importance of low- and high-latitude temperature changes, *JGR atmospheres*, **110 (D12)**, Art. No. D12108.
- Roeckner, E., K. Arpe, L. Bengtsson, M. Christoph, M. Claussen, L. Dümenil, M. Esch, M. Giorgetta, U. Schlese and U. Schulzweida, 1996: The atmospheric general circulation model ECHAM4: Model description and simulation of present-day climate. MPI Report No. 218, Max-Planck-Institut für Meteorologie, Hamburg, Germany, 90pp.
- Rogers, J. C., and H. van Loon, 1982. Spatial Variability of Sea Level Pressure and 500mb height anomalies over the southern hemisphere. *Mon. Weath. Rev.*, **110**, 1375-1392.
- Schmutz, C., D. Gyalistras, J. Luterbacher, and H. Wanner, 2001. Reconstruction of monthly 700. 500 and 300 hPa geopotential height fields in the European and Eastern North Atlantic region for the period 1901-1947. *Clim. Res.*, **18**, 181-193.
- Schmutz, C., J. Luterbacher, D. Gyalistras, E. Xoplake, and H. Wanner, 2000. Can we trust proxy-based NAO index reconstructions? *Geophys. Res. Lett.*, **27**, 1135-1138.
- Schneider, D. P., E. J. Steig, J. M. Jones, T. D. van Ommen and D. Dixon, 2004. Ice core evidence of 200 years of Antarctic climate change and its connections with the Southern Annular Mode. Bjerkenes Centenary 2004 Open Science Conference, Climate Change in High Latitudes, Bergen.
- Schweingruber, F H, K R Briffa, and P D Jones, 1991: Yearly maps of summer temperatures in Western Europe from AD 1750 to 1975 and western North-America from 1600 to 1982 - results of a radiodensitometrical study from tree rings. *Vegetatio*, **92**, 5-71.
- Shindell, D. T., G.A. Schmidt, M. E. Mann, D. Rind, A. Waple, 2001. Solar forcing of regional climate change during the maunder minimum. *Science*, **294**, 2149-2152.
- Slonosky et al. 1999, Homogenization techniques for European monthly mean surface pressure time

series, *J. Climate*, **12**, 2658-2672.

Stone, D. A., A. J. Weaver and R. J. Stouffer, 2001. Projection of climate change onto modes of atmospheric variability. *J. Climate*, **14**, 3551-3565.

Swinbank, R., V. Shutyaev and W.A. Lahoz, 2003. Data Assimilation for the Earth System. Nato Science Series IV, **26**, 377 pp. Kluwer Academic Publishers.

Thompson, D. W. J. and S. Solomon, 2002. Interpretation of recent Southern Hemisphere climate change. *Science*, **296**, 895-899.

Thompson, D. W. J., and J. M. Wallace, 2000. Annular modes in the extratropical circulation. Part I: month-to-month variability, *J. Climate*, **13**, 1000-1016.

Thompson, D. W. J., J. M. Wallace, and G. C. Hegerl, 2000. Annular modes in the extratropical circulation. Part II: Trends. *J. Climate*, **13**, 1018-1035.

Timm., O, E. Ruprecht, and S. Kleppek, 2004. Scale-dependent reconstruction of the NAO index. *J. Clim.*, **16**, 27-39.

Timmreck, C., H. F. Graf and J. Feichter, 1999: Simulation of the Mt. Pinatubo volcanic aerosol with the Hamburg climate model ECHAM4. *Theor. Appl. Climatol.*, **62**, 85-108.

Trenberth, K. E. and D. A. Paolino, 1980. The Northern Hemisphere Sea-Level Pressure Data Set – Trends, Errors and Discontinuities. *Mon. Weath. Rev.*, **108**, 855-872.

Van der Schrier, G., and Barkmeijer, J., 2005. Bjerknes' hypothesis on the coldness during AD 1790-1820 revisited. *Clim. Dyn.*, **24**, 355-371.

von Storch, H. and F. W. Zwiers, 1999. Statistical analysis in climate research. Cambridge University Press.

Von Storch, H., U. Cubasch, J. F. Gonzalez-Rouco, J. M. Jones, R. Voss, M. Widmann, and E. Zorita, 2000a. Combining paleoclimatic evidence and GCMs by means of data assimilation through upscaling and nudging (DATUN). *Proc. 11th Symposium on global change studies*, AMS, Long Beach, CA. 28-31.

Von Storch, H., H. Langenberg and F. Feser, 2000b. A spectral nudging technique for dynamical downscaling purposes. *Mon. Weather. Rev.*, **128**, 3664-3673.

Widmann, M., 2005. One-dimensional CCA and SVD, and their relationship to regression maps. *J. Climate*, **18**, 2785-2792.

Widmann, M., H. Von Storch, R. Schnur, and I. Kirchner, 2005. Assimilation of large-scale circulation states into the ECHAM4 atmospheric GCM with pattern nudging. *Clim. Dyn.*, in preparation.

Widmann, M., J.M. Jones and H. von Storch, 2004. Reconstruction of large-scale atmospheric circulation and data assimilation in paleoclimatology. *Pages Newsletter*, **12**(2), 12-13.

Widmann, M., C. S. Bretherton, and E. P. Salathé Jr., 2003: Statistical precipitation downscaling over the Northwestern United States using numerically simulated precipitation as a predictor. *J. Clim*, **16**, 799-816.

Wolff, J. –O, E. Maier-Reimer, and S. Legutke, 1997. The Hamburg Ocean Primitive Equation Model. Technical report No. 13, German Climate Computing Center (DKRZ), Hamburg.

Zorita, E, H. von Storch, J. F. González-Rouco, U. Cubasch, J. Luterbacher, S. Legutke, I. Fischer-Bruns, and U. Schlese, 2004. Climate evolution in the last five centuries simulated by an atmosphere-ocean model: global temperatures, the North Atlantic Oscillation and the Late Maunder Minimum. *Meteorologische Zeitschrift* 13, 271.

Zorita, E. and F. González-Rouco, 2002. Are temperature-sensitive proxies adequate for North Atlantic Oscillation reconstructions?. *Geophysical Research Letters*, **29**, 48-1 - 48-4.

Zorita, E., F. González-Rouco, and S. Legutke, 2003. Testing the Mann et al. (1998) Approach to Paleoclimate Reconstructions in the Context of a 1000-Yr Control Simulation with the ECHO-G Coupled Climate Model . *J. Climate*, **16**,1378-1390.

Zorita, E. and, H.von Storch, 1999. The analog method as a simple statistical downscaling technique:comparison with more complicated methods. *J. Climate*, **12**, 2474-2489.